Geodesic Methods in Computer Vision and Graphics

Geodesic Methods in Computer Vision and Graphics

Gabriel Peyré

Université Paris-Dauphine, France
peyre@ceremade.dauphine.fr

Mickael Péchaud

École Normale Supérieure, France
mickael.pechaud@normalesup.org

Renaud Keriven

École des Ponts ParisTech, France
keriven@imagine.enpc.fr

Laurent D. Cohen

Université Paris-Dauphine, France
cohen@ceremade.dauphine.fr

the essence of knowledge

Boston – Delft

Foundations and Trends® in Computer Graphics and Vision

Published, sold and distributed by:
now Publishers Inc.
PO Box 1024
Hanover, MA 02339
USA
Tel. +1-781-985-4510
www.nowpublishers.com
sales@nowpublishers.com

Outside North America:
now Publishers Inc.
PO Box 179
2600 AD Delft
The Netherlands
Tel. +31-6-51115274

The preferred citation for this publication is G. Peyré, M. Péchaud, R. Keriven and L. D. Cohen, Geodesic Methods in Computer Vision and Graphics, Foundations and Trends® in Computer Graphics and Vision, vol 5, nos 3–4, pp 197–397, 2009

ISBN: 978-1-60198-396-1

Editorial Scope

Foundations and Trends® in Computer Graphics and Vision will publish survey and tutorial articles in the following topics:

- Rendering: Lighting models; Forward rendering; Inverse rendering; Image-based rendering; Non-photorealistic rendering; Graphics hardware; Visibility computation
- Shape: Surface reconstruction; Range imaging; Geometric modelling; Parameterization;
- Mesh simplification
- Animation: Motion capture and processing; Physics-based modelling; Character animation
- Sensors and sensing
- Image restoration and enhancement
- Segmentation and grouping
- Feature detection and selection
- Color processing
- Texture analysis and synthesis
- Illumination and reflectance modeling
- Shape Representation
- Tracking
- Calibration
- Structure from motion
- Motion estimation and registration
- Stereo matching and reconstruction
- 3D reconstruction and image-based modeling
- Learning and statistical methods
- Appearance-based matching
- Object and scene recognition
- Face detection and recognition
- Activity and gesture recognition
- Image and Video Retrieval
- Video analysis and event recognition
- Medical Image Analysis
- Robot Localization and Navigation

Information for Librarians

Foundations and Trends® in Computer Graphics and Vision, 2009, Volume 5, 4 issues. ISSN paper version 1572-2740. ISSN online version 1572-2759. Also available as a combined paper and online subscription.

Foundations and Trends® in
Computer Graphics and Vision
Vol. 5, Nos. 3–4 (2009) 197–397

DOI: 10.1561/0600000029

Geodesic Methods in Computer Vision and Graphics

Gabriel Peyré[1], Mickael Péchaud[2], Renaud Keriven[3], and Laurent D. Cohen[4]

[1] *Ceremade, UMR CNRS 7534, Université Paris-Dauphine, Place de Lattre de Tassigny, Paris Cedex 16, 75775, France, peyre@ceremade.dauphine.fr*
[2] *DI École Normale Supérieure, 45 rue d'Ulm, Paris, 75005, France, mickael.pechaud@normalesup.org*
[3] *IMAGINE-LIGM, École des Ponts ParisTech, 6 av Blaise Pascal, Marne-la-Valle, 77455, France, keriven@imagine.enpc.fr*
[4] *Ceremade, UMR CNRS 7534, Université Paris-Dauphine, Place de Lattre de Tassigny, Paris Cedex 16, 75775, France, cohen@ceremade.dauphine.fr*

Abstract

This monograph reviews both the theory and practice of the numerical computation of geodesic distances on Riemannian manifolds . The notion of Riemannian manifold allows one to define a local metric (a symmetric positive tensor field) that encodes the information about the problem one wishes to solve. This takes into account a local isotropic cost (whether some point should be avoided or not) and a local anisotropy (which direction should be preferred). Using this local tensor field, the geodesic distance is used to solve many problems of practical interest such as segmentation using geodesic balls and Voronoi regions, sampling points at regular geodesic distance or meshing a domain with

geodesic Delaunay triangles. The shortest paths for this Riemannian distance, the so-called geodesics, are also important because they follow salient curvilinear structures in the domain. We show several applications of the numerical computation of geodesic distances and shortest paths to problems in surface and shape processing, in particular segmentation, sampling, meshing and comparison of shapes. All the figures from this review paper can be reproduced by following the Numerical Tours of Signal Processing.

`http://www.ceremade.dauphine.fr/∼peyre/numerical-tour/`

Several textbooks exist that include description of several manifold methods for image processing, shape and surface representation and computer graphics. In particular, the reader should refer to [42, 147, 208, 209, 213, 255] for fascinating applications of these methods to many important problems in vision and graphics. This review paper is intended to give an updated tour of both foundations and trends in the area of geodesic methods in vision and graphics.

Contents

1

Theoretical Foundations of Geodesic Methods

This section introduces the notion of Riemannian manifold that is a unifying setting for all the problems considered in this review paper. This notion requires only the design of a local metric, which is then integrated over the whole domain to obtain a distance between pairs of points. The main property of this distance is that it satisfies a non-linear partial differential equation, which is at the heart of the fast numerical schemes considered in Section 2.

1.1 Two Examples of Riemannian Manifolds

To give a flavor of Riemannian manifolds and geodesic paths, we give two important examples in computer vision and graphics.

1.1.1 Tracking Roads in Satellite Image

An important and seminal problem in computer vision consists in detecting salient curves in images, see for instance [57]. They can be used to perform segmentation of the image, or track features. A representative example of this problem is the detection of roads in satellite images.

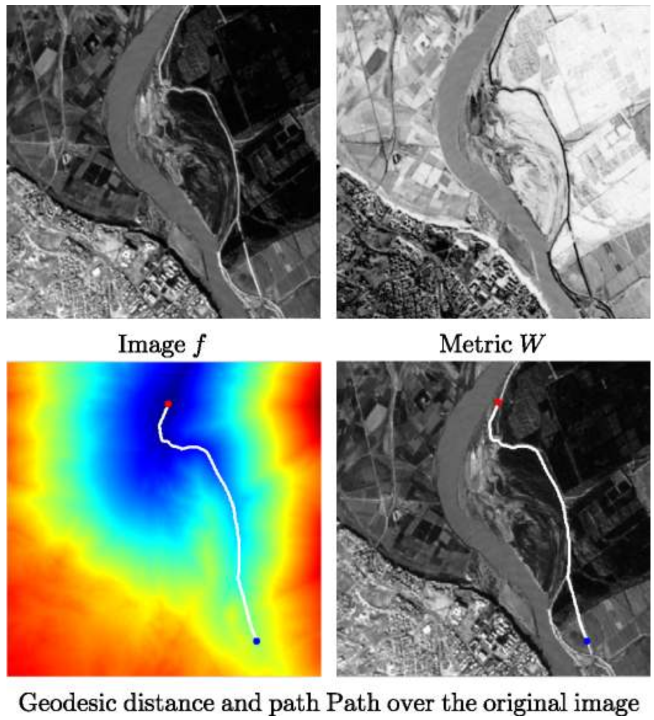

Fig. 1.1 Example of geodesic curve extracted using the weighted metric (1.1). x_s and x_e correspond, respectively, to the red and blue points.

Figure 1.1, upper left, displays an example of satellite image f, that is modeled as a 2D function $f\colon\Omega \to \mathbb{R}$, where the image domain is usually $\Omega = [0,1]^2$. A simple model of road is that it should be approximately of constant gray value $c \in \mathbb{R}$. One can thus build a saliency map $W(x)$ that is low in area where there is a high confidence that some road is passing by, as suggested for instance in [72]. As an example, one can define

$$W(x) = |f(x) - c| + \varepsilon \tag{1.1}$$

where ε is a small value that prevents $W(x)$ from vanishing.

Using this saliency map, one defines the length of a smooth curve on the image $\gamma\colon[0,1] \to \Omega$ as a weighted length

$$L(\gamma) = \int_0^1 W(\gamma(t))\|\gamma'(t)\|\mathrm{d}t \tag{1.2}$$

where $\gamma'(t) \in \mathbb{R}^2$ is the derivative of γ. We note that this measure of lengths extends to piecewise smooth curves by splitting the integration into pieces where the curve is smooth.

The length $L(\gamma)$ is smaller when the curve passes by regions where W is small. It thus makes sense to declare as roads the curves that minimize $L(\gamma)$. For this problem to make sense, one needs to further constrain γ. And a natural choice is to fix its starting and ending points to be a pair $(x_s, x_e) \in \Omega^2$

$$\mathcal{P}(x_s, x_e) = \{\gamma : [0,1] \to \Omega \setminus \gamma(0) = x_s \quad \text{and} \quad \gamma(1) = x_e\}, \tag{1.3}$$

where the paths are assumed to be piecewise smooth so that one can measure their lengths using (1.2).

Within this setting, a road $\gamma^\star$ is a global minimizer of the length

$$\gamma^\star = \underset{\gamma \in \mathcal{P}(x_s, x_e)}{\operatorname{argmin}} L(\gamma), \tag{1.4}$$

which in general exists, and is unique except in degenerate situations where different roads have the same length. Length $L(\gamma^\star)$ is called geodesic distance between x_s and x_e with respect to $W(x)$.

Figure 1.1 shows an example of geodesic extracted with this method. It links two points x_s and x_e given by the user. One can see that this curve tends to follow regions with gray values close to c, which has been fixed to $c = f(x_e)$.

This idea of using a scalar potential $W(x)$ to weight the length of curves has been used in many computer vision applications beside road tracking. This includes in particular medical imaging where one wants to extract contours of organs or blood vessels. These applications are further detailed in Section 3.

1.1.2 Detecting Salient Features on Surfaces

Computer graphics applications often face problems that require the extraction of meaningful curves on surfaces. We consider here a smooth surface $\mathcal{S}$ embedded into the 3D Euclidean space, $\mathcal{S} \subset \mathbb{R}^3$.

Similarly to (1.2), a curve $\tilde{\gamma}: [0,1] \to \mathcal{S}$ traced on the surface has a weighted length computed as

$$L(\tilde{\gamma}) = \int_0^1 W(\tilde{\gamma}(t)) \|\tilde{\gamma}'(t)\| \mathrm{d}t, \tag{1.5}$$

where $\tilde{\gamma}'(t) \in \mathcal{T}_{\tilde{\gamma}(t)} \subset \mathbb{R}^3$ is the derivative vector, that lies in the embedding space $\mathbb{R}^3$, and is in fact a vector belonging to the 2D tangent plane $\mathcal{T}_{\tilde{\gamma}(t)}$ to the surface at $\tilde{\gamma}(t)$, and the weight W is a positive function defined on the surface domain $\mathcal{S}$.

Note that we use the notation $\tilde{x} = \tilde{\gamma}(t)$ to insist on the fact that the curves are not defined in a Euclidean space, and are forced to be traced on a surface.

Similarly to (1.4), a geodesic curve

$$\tilde{\gamma}^\star = \underset{\tilde{\gamma} \in \mathcal{P}(\tilde{x}_s, \tilde{x}_e)}{\operatorname{argmin}} \; L(\tilde{\gamma}), \tag{1.6}$$

is a shortest curve joining two points $\tilde{x}_s, \tilde{x}_e \in \mathcal{S}$.

When $W = 1$, $L(\tilde{\gamma})$ is simply the length of a 3D curve, that is restricted to be on the surface $\mathcal{S}$. Figure 1.2 shows an example of surface, together with a set of geodesics joining pairs of points, for $W = 1$. As detailed in Section 3.2.4, a varying saliency map $W(\tilde{x})$ can be defined from a texture or from the curvature of the surface to detect salient curves.

Geodesics and geodesic distance on 3D surfaces have found many applications in computer vision and graphics, for example, surface matching, detailed in Section 5, and surface remeshing, detailed in Section 4.

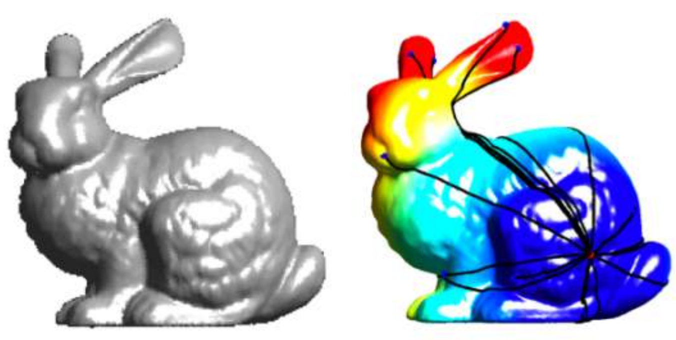

Fig. 1.2 Example of geodesic curves on a 3D surface.

1.2 Riemannian Manifolds

It turns out that both previous examples can be cast into the same general framework using the notion of a Riemannian manifold of dimension 2.

1.2.1 Surfaces as Riemannian Manifolds

Although the curves described in Sections 1.1.1 and 1.1.2 do not belong to the same spaces, it is possible to formalize the computation of geodesics in the same way in both cases. In order to do so, one needs to introduce the Riemannian manifold $\Omega \subset \mathbb{R}^2$ associated to the surface $\mathcal{S}$ [148].

A smooth surface $\mathcal{S} \subset \mathbb{R}^3$ can be locally described as a parametric function

$$\varphi : \begin{array}{ccc} \Omega \subset \mathbb{R}^2 & \to & \mathcal{S} \subset \mathbb{R}^3 \\ x & \mapsto & \tilde{x} = \varphi(x) \end{array} \tag{1.7}$$

which is required to be differentiable and one-to-one, where Ω is an open domain of $\mathbb{R}^2$.

Full surfaces require several such mappings to be fully described, but we postpone this difficulty until Section 1.2.2.

The tangent plane $\mathcal{T}_{\tilde{x}}$ at a surface point $\tilde{x} = \varphi(x)$ is spanned by the two partial derivatives of the parameterization, which define the derivative matrix at point $x = (x_1, x_2)$

$$D\varphi(x) = \left(\frac{\partial \varphi}{\partial x_1}(x), \frac{\partial \varphi}{\partial x_2}(x) \right) \in \mathbb{R}^{3\times 2}. \tag{1.8}$$

As shown in Figure 1.3, the derivative of any curve $\tilde{\gamma}$ at a point $\tilde{x} = \tilde{\gamma}(t)$ belongs to the tangent plane $\mathcal{T}_{\tilde{x}}$ of $\mathcal{S}$ at $\tilde{x}$.

The curve $\tilde{\gamma}(t) \in \mathcal{S} \subset \mathbb{R}^3$ defines a curve $\gamma(t) = \varphi^{-1}(\tilde{\gamma}(t)) \in \Omega$ traced on the parameter domain. Note that while $\tilde{\gamma}$ belongs to a curved surface, γ is traced on a subset of a Euclidean domain.

Since $\tilde{\gamma}(t) = \varphi(\gamma(t)) \in \Omega$ the tangents to the curves are related via $\tilde{\gamma}'(t) = D\varphi(\gamma(t))\gamma'(t)$ and $\tilde{\gamma}'(t)$ is in the tangent plane $\mathcal{T}_{\tilde{\gamma}(t)}$ which is spanned by the columns of $D\varphi(\gamma(t))$. The length (1.5) of the curve $\tilde{\gamma}$

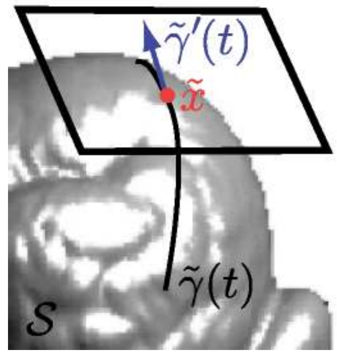

Fig. 1.3 Tangent space $\mathcal{T}_{\tilde{x}}$ and derivative of a curve on surface $\mathcal{S}$.

is computed as

$$L(\tilde{\gamma}) = L(\gamma) = \int_0^1 \|\gamma'(t)\|_{T_{\gamma(t)}} \mathrm{d}t, \tag{1.9}$$

where the tensor T_x is defined as

$$\forall\, x \in \Omega, \quad T_x = \sqrt{W(\tilde{x})} I_\varphi(x) \quad \text{where } \tilde{x} = \varphi(x),$$

and $I_\varphi(x) \in \mathbb{R}^{2\times 2}$ is the first fundamental form of $\mathcal{S}$

$$I_\varphi(x) = (D\varphi(x))^{\mathrm{T}} D\varphi(x) = \left(\left\langle \frac{\partial \varphi}{\partial x_i}(x) \frac{\partial \varphi}{\partial x_j}(x) \right\rangle \right)_{1\leq i,j\leq 2} \tag{1.10}$$

and where, given some positive symmetric matrix $A = (A_{i,j})_{1\leq i,j\leq 2} \in \mathbb{R}^{2\times 2}$, we define its associated norm

$$\|u\|_A^2 = \langle u, u\rangle_A \quad \text{where } \langle u, v\rangle_A = \langle Au, v\rangle = \sum_{1\leq i,j\leq 2} A_{i,j} u_i v_j. \tag{1.11}$$

A domain Ω equipped with such a metric is called a Riemannian manifold.

The geodesic curve $\tilde{\gamma}^\star$ traced on the surface $\mathcal{S}$ defined in (1.6) can equivalently be viewed as a geodesic $\gamma^\star = \varphi^{-1}(\tilde{\gamma}^\star)$ traced on the Riemannian manifold Ω. While $\tilde{\gamma}^\star$ minimizes the length (1.5) in the 3D embedding space between $\tilde{x}_s$ and $\tilde{x}_e$ the curve $\gamma^\star$ minimizes the Riemannian length (1.9) between $x_s = \varphi^{-1}(\tilde{x}_s)$ and $x_e = \varphi^{-1}(\tilde{x}_e)$.

1.2.2 Riemannian Manifold of Arbitrary Dimensions

Local description of a manifold without boundary. We consider an arbitrary manifold $\mathcal{S}$ of dimension d embedded in $\mathbb{R}^n$ for some $n \geq d$ [164]. This generalizes the setting of the previous Section 1.2.1 that considers $d = 2$ and $n = 3$. The manifold is assumed for now to be closed, which means without boundary.

As already done in (1.7), the manifold is described locally using a bijective smooth parametrization

$$\varphi: \begin{array}{ccc} \Omega \subset \mathbb{R}^d & \rightarrow & \mathcal{S} \subset \mathbb{R}^n \\ x & \mapsto & \tilde{x} = \varphi(x) \end{array}$$

so that $\varphi(\Omega)$ is an open subset of $\mathcal{S}$.

All the objects we consider, such as curves and length, can be transposed from $\mathcal{S}$ to Ω using this application. We can thus restrict our attention to Ω, and do not make any reference to the surface $\mathcal{S}$.

For an arbitrary dimension d, a Riemannian manifold is thus locally described as a subset of the ambient space $\Omega \subset \mathbb{R}^d$, having the topology of an open sphere, equipped with a positive definite matrix $T_x \in \mathbb{R}^{d \times d}$ for each point $x \in \Omega$, that we call a tensor field. This field is further required to be smooth.

Similarly to (1.11), at each point $x \in \Omega$, the tensor T_x defines the length of a vector $u \in \mathbb{R}^d$ using

$$\|u\|_{T_x}^2 = \langle u, u \rangle_{T_x} \quad \text{where } \langle u, v \rangle_{T_x} = \langle T_x u, v \rangle = \sum_{1 \leq i,j \leq d} (T_x)_{i,j} u_i v_j.$$

This allows one to compute the length of a curve $\gamma(t) \in \Omega$ traced on the Riemannian manifold as a weighted length where the infinitesimal length is measured according to T_x

$$L(\gamma) = \int_0^1 \|\gamma'(t)\|_{T_{\gamma(t)}} \mathrm{d}t. \tag{1.12}$$

The weighted metric on the image for road detection defined in Section 1.1.1 fits within this framework for $d = 2$ by considering $\Omega = [0,1]^2$ and $T_x = W(x)^2 \mathrm{Id}_2$, where $\mathrm{Id}_2 \in \mathbb{R}^{2 \times 2}$ is the identity matrix. In this case, $\Omega = \mathcal{S}$, and φ is the identity application. The parameter domain metric defined from a surface $\mathcal{S} \subset \mathbb{R}^3$ considered in Section 1.1.2 can also be viewed as a Riemannian metric as we explained in the previous section.

Global description of a manifold without boundary. The local description of the manifold as a subset $\Omega \subset \mathbb{R}^d$ of an Euclidean space is only able to describe parts that are topologically equivalent to open spheres.

A manifold $\mathcal{S} \in \mathbb{R}^n$ embedded in $\mathbb{R}^n$ with an arbitrary topology is decomposed using a finite set of overlapping surfaces $\{\mathcal{S}_i\}_i$ topologically equivalent to open spheres such that

$$\bigcup_i \mathcal{S}_i = \mathcal{S}. \tag{1.13}$$

A chart $\varphi_i : \{\Omega_i\}_i \to \mathcal{S}_i$ is defined for each of sub-surface $\mathcal{S}_i$.

Figure 1.4 shows how a 1D circle is locally parameterized using several 1D segments.

Manifolds with boundaries. In applications, one often encounters manifolds with boundaries, for instance images defined on a square, volume of data defined inside a cube, or planar shapes.

The boundary $\partial\Omega$ of a manifold Ω of dimension d is itself by definition a manifold of dimension $d-1$. Points x strictly inside the manifold are assumed to have a local neighborhood that can be parameterized over a small Euclidean ball. Points located on the boundary are parameterized over a half Euclidean ball.

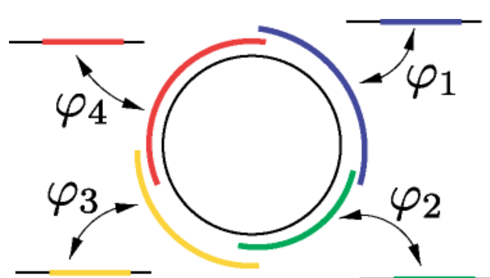

Fig. 1.4 The circle is a 1-dimensional surface embedded in $\mathbb{R}^2$, and is thus a 1D manifold. In this example, it is decomposed in four sub-surfaces which are topologically equivalent to sub-domains of $\mathbb{R}$, through charts φ_i.

Such manifolds require some extra mathematical care, since geodesic curves (local length minimizers) and shortest paths (global length minimizing curves), defined in Section 1.2.3, might exhibit tangential discontinuities when reaching the boundary of the manifold.

Note however that these curves can still be computed numerically as described in Section 2. Note also that the characterization of the geodesic distance as the viscosity solution of the Eikonal equation still holds for manifolds with boundary.

1.2.3 Geodesic Curves

Globally minimizing shortest paths. Similarly to (1.4), one defines a geodesic $\gamma^\star(t) \in \Omega$ between two points $(x_s, x_e) \in \Omega^2$ as the curve between x_s and x_e with minimal length according to the Riemannian metric (1.9):

$$\gamma^\star = \underset{\gamma \in \mathcal{P}(x_s, x_e)}{\operatorname{argmin}} \; L(\gamma). \tag{1.14}$$

As an example, in the case of a uniform $T_x = Id_d$ (i.e., the metric is Euclidean) and a convex Ω, the unique geodesic curve between x_s and x_e is the segment joining the two points.

Existence of shortest paths between any pair of points on a connected Riemannian manifold is guaranteed by the Hopf-Rinow theorem [134]. Such a curve is not always unique, see Figure 1.5.

Locally minimizing geodesic curves. It is important to note that in this paper the notion of geodesics refers to minimal paths, that

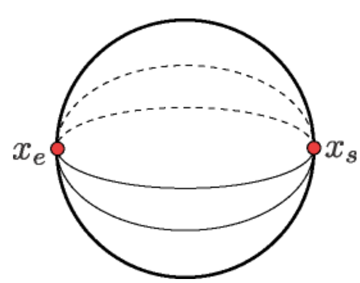

Fig. 1.5 Example of non-uniqueness of a shortest path between two points: there is an infinite number of shortest paths between two antipodal points on a sphere.

are curves minimizing globally the Riemannian length between two points. In contrast, the mathematical definition of geodesic curves usually refers to curves that are local minimizer of the geodesic lengths. These locally minimizing curves are the generalization of straight lines in Euclidean geometry to the setting of Riemannian manifolds.

Such a locally minimizing curve satisfies an ordinary differential equation, that expresses that it has a vanishing Riemannian curvature.

There might exist several local minimizers of the length between two points, which are not necessarily minimal paths. For instance, on a sphere, a great circle passing by two points is composed of two local minimizer of the length, and only one of the two portion of circle is a minimal path.

1.2.4 Geodesic Distance

The geodesic distance between two points x_s, x_e is the length of $\gamma^\star$.

$$d(x_s, x_e) = \min_{\gamma \in \mathcal{P}(x_s, x_e)} L(\gamma) = L(\gamma^\star). \tag{1.15}$$

This defines a metric on Ω, which means that it is symmetric $d(x_s, x_e) = d(x_e, x_s)$, that $d(x_s, x_e) > 0$ unless $x_s = x_e$ and then $d(x_s, x_e) = 0$, and that it satisfies the triangular inequality for every point y

$$d(x_s, x_e) \leq d(x_s, y) + d(y, x_e).$$

The minimization (1.15) is thus a way to transfer a local metric defined point-wise on the manifold Ω into a global metric that applies to arbitrary pairs of points on the manifold.

This metric $d(x_s, x_e)$ should not be mistaken for the Euclidean metric $\|x_s - x_e\|$ on $\mathbb{R}^n$, since they are in general very different. As an example, if r denotes the radius of the sphere in Figure 1.5, the Euclidean distance between two antipodal points is $2r$ while the geodesic distance is πr.

1.2.5 Anisotropy

Let us assume that Ω is of dimension 2. To analyze locally the behavior of a general anisotropic metric, the tensor field is diagonalized as

$$T_x = \lambda_1(x) e_1(x) e_1(x)^{\mathrm{T}} + \lambda_2(x) e_2(x) e_2(x)^{\mathrm{T}}, \tag{1.16}$$

where $0 < \lambda_1(x) \leq \lambda_2(x)$. The vector fields $e_i(x)$ are orthogonal eigenvectors of the symmetric matrix T_x with corresponding eigenvalues $\lambda_i(x)$. The norm of a tangent vector $v = \gamma'(t)$ of a curve at a point $x = \gamma(t)$ is thus measured as

$$\|v\|_{T_x} = \lambda_1(x)|\langle e_1(x), v\rangle|^2 + \lambda_2(x)|\langle e_2(x), v\rangle|^2.$$

A curve γ is thus locally shorter near x if its tangent $\gamma'(t)$ is collinear to $e_1(x)$, as shown in Figure 1.6. Geodesic curves thus tend to be as parallel as possible to the eigenvector field $e_1(x)$. This diagonalization (1.16) carries over to arbitrary dimension d by considering a family of d eigenvector fields.

For image analysis, in order to find significant curves as geodesics of a Riemannian metric, the eigenvector field $e_1(x)$ should thus match the orientation of edges or of textures, as this is the case for Figure 1.7, right.

The strength of the directionality of the metric is measured by its anisotropy $A(x)$, while its global isotropic strength is measured using its energy $W(x)$

$$A(x) = \frac{\lambda_2(x) - \lambda_1(x)}{\lambda_2(x) + \lambda_1(x)} \in [0,1] \quad \text{and} \quad W(x)^2 = \frac{\lambda_2(x) + \lambda_1(x)}{2} > 0. \tag{1.17}$$

A tensor field with $A(x) = 0$ is isotropic and thus verifies $T_x = W(x)^2 \mathrm{Id}_2$, which corresponds to the setting considered in the road tracking application of Section 1.1.1.

Figure 1.7 shows examples of metric with a constant energy $W(x) = W$ and an increasing anisotropy $A(x) = A$. As the anisotropy

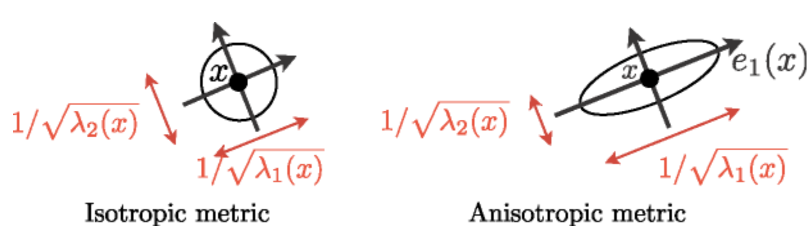

Fig. 1.6 Schematic display of a local geodesic ball for an isotropic metric or an anisotropic metric.

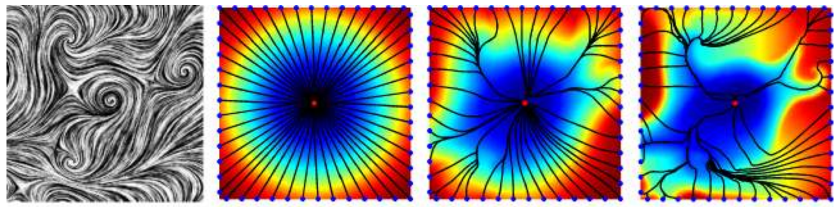

Fig. 1.7 Example of geodesic distance to the center point, and geodesic curves between this center point and points along the boundary of the domain. These are computed for a metric with an increasing value of anisotropy A, and for a constant W. The metric is computed from the image f using (4.37).

A drops to 0, the Riemannian manifold comes closer to Euclidean, and geodesic curves become line segments.

1.3 Other Examples of Riemannian Manifolds

One can find many occurrences of the notion of Riemannian manifold to solve various problems in computer vision and graphics. All these methods build, as a pre-processing step, a metric T_x suited for the problem to solve, and use geodesics to integrate this local distance information into globally optimal minimal paths. Figure 1.8 synthesizes different possible Riemannian manifolds. The last two columns correspond to examples already considered in Sections 1.1.1 and 1.2.5.

1.3.1 Euclidean Distance

The classical Euclidean distance $d(x_s, x_e) = \|x_s - x_e\|$ in $\Omega = \mathbb{R}^d$ is recovered by using the identity tensor $T_x = \mathrm{Id}_d$. For this identity metric, shortest paths are line segments. Figure 1.8, first column, shows this simple setting. This is generalized by considering a constant metric $T_x = T \in \mathbb{R}^{2\times 2}$, in which case the Euclidean metric is measured according to T, since $d(x_s, x_e) = \|x_s - x_e\|_T$. In this setting, geodesics between two points are straight lines.

1.3.2 Planar Domains and Shapes

If one uses a locally Euclidean metric $T_x = \mathrm{Id}_2$ in 2D, but restricts the domain to a non-convex planar compact subset $\Omega \subset \mathbb{R}^2$, then

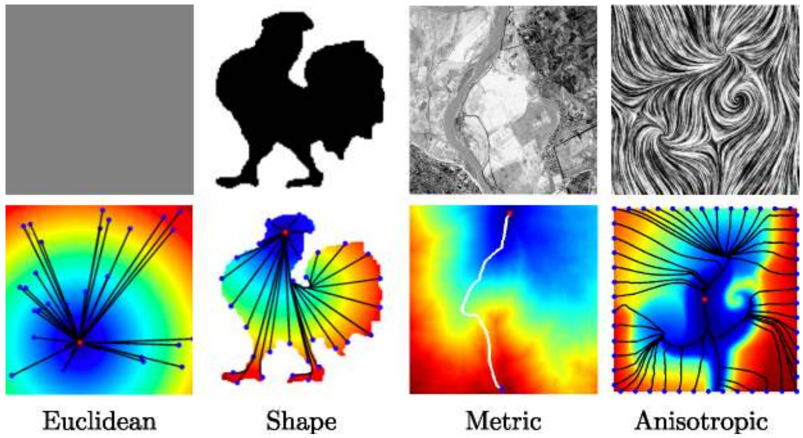

Fig. 1.8 Examples of Riemannian metrics (top row), geodesic distances and geodesic curves (bottom row). The blue/red color-map indicates the geodesic distance to the starting red point. From left to right: Euclidean ($T_x = \mathrm{Id}_2$ restricted to $\Omega = [0,1]^2$), planar domain ($T_x = \mathrm{Id}_2$ restricted to $\mathcal{M} \subset [0,1]^2$), isotropic metric ($\Omega = [0,1]^2$, $T(x) = W(x)Id_2$, see Equation (1.1)), Riemannian manifold metric (T_x is the structure tensor of the image, see Equation (4.37)).

the geodesic distance $d(x_s, x_e)$ might differ from the Euclidean length $\|x_s - x_e\|$. This is because paths are restricted to lie inside Ω, and some shortest paths are forced to follow the boundary of the domain, thus deviating from line segment (see Figure 1.8, second column).

This shows that the global integration of the local length measure T_x to obtain the geodesic distance $d(x_s, x_e)$ takes into account global geometrical and topological properties of the domain. This property is useful to perform shape recognition, that requires some knowledge of the global structure of a shape $\Omega \subset \mathbb{R}^2$, as detailed in Section 5.

Such non-convex domain geodesic computation also found application in robotics and video games, where one wants to compute an optimal trajectory in an environment consisting of obstacles, or in which some positions are forbidden [153, 161]. This is detailed in Section 3.6.

1.3.3 Anisotropic Metric on Images

Section 1.1.1 detailed an application of geodesic curve to road tracking, where the Riemannian metric is a simple scalar weight computed from some image f. This weighting scheme does not take advantage of the local orientation of curves, since the metric $W(x)\|\gamma'(t)\|$ is only sensitive to the amplitude of the derivative.

One can improve this by computing a 2D tensor field T_x at each pixel location $x \in \mathbb{R}^{2\times 2}$. The precise definition of this tensor depends on the precise applications, see Section 3.2. They generally take into account the gradient $\nabla f(x)$ of the image f around the pixel x, to measure the local directionality of the edges or the texture. Figure 1.8, right, shows an example of metric designed to match the structure of a texture.

1.4 Voronoi Segmentation and Medial Axis

1.4.1 Voronoi Segmentation

For a finite set $S = \{x_i\}_{i=0}^{K-1}$ of starting points, one defines a segmentation of the manifold Ω into Voronoi cells

$$\Omega = \bigcup_i \mathcal{C}_i \quad \text{where } \mathcal{C}_i = \{x \in \Omega \setminus \forall j \neq i,\ d(x,x_j) \geq d(x,x_i)\}. \quad (1.18)$$

Each region $\mathcal{C}_i$ can be interpreted as a region of influence of x_i. Section 2.6.1 details how to compute this segmentation numerically, and Section 4.1.1 discusses some applications.

This segmentation can also be represented using a partition function

$$\ell(x) = \underset{0\leq i<K}{\operatorname{argmin}}\, d(x,x_i). \quad (1.19)$$

For points x which are equidistant from at least two different starting points x_i and x_j, i.e., $d(x,x_i) = d(x,x_j)$, one can pick either $\ell(x) = i$ or $\ell(x) = j$. Except for these exceptional points, one thus has $\ell(x) = i$ if and only if $x \in \mathcal{C}_i$.

Figure 1.9, top row, shows an example of Voronoi segmentation for an isotropic metric.

This partition function $\ell(x)$ can be extended to the case where S is not a discrete set of points, but for instance the boundary of a 2D shape. In this case, $\ell(x)$ is not integer valued but rather indicates the location of the closest point in S. Figure 1.9, bottom row, shows an example for a Euclidean metric restricted to a non-convex shape, where S is the boundary of the domain. In the third image, the colors are mapped to the points of the boundary S, and the color of each point x corresponds to the one associated with $\ell(x)$.

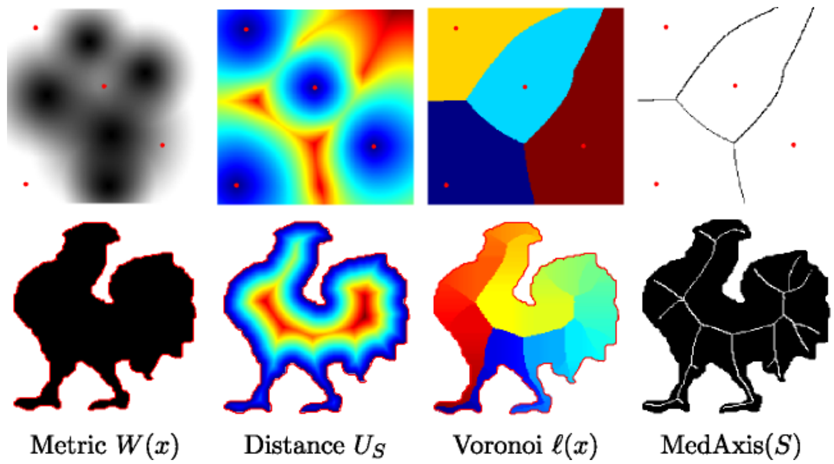

Fig. 1.9 Examples of distance function, Voronoi segmentation and medial axis for an isotropic metric (top left) and a constant metric inside a non-convex shape (bottom left).

1.4.2 Medial Axis

The medial axis is the set of points where the distance function U_S is not differentiable. This corresponds to the set of points $x \in \Omega$ where two distinct shortest paths join x to S.

The major part of the medial axis is thus composed of points that are at the same distance from two points in S

$$\left\{ x \in \Omega \setminus \exists (x_1, x_2) \in S^2 \middle| \begin{array}{l} x_1 \neq x_2 \\ d(x, x_1) = d(x, x_2) \end{array} \right\} \subset \mathrm{MedAxis}(S). \quad (1.20)$$

This inclusion might be strict because it might happen that two points $x \in \Omega$ and $y \in S$ are linked by two different geodesics.

Finite set of points. For a discrete finite set $S = \{x_i\}_{i=0}^{N-1}$, a point x belongs to MedAxis(S) either if it is on the boundary of a Voronoi cell, or if two distinct geodesics are joining x to a single point of S. One thus has the inclusion

$$\bigcup_{x_i \in S} \partial \mathcal{C}_i \subset \mathrm{MedAxis}(S) \quad (1.21)$$

where $\mathcal{C}_i$ is defined in (1.18).

For instance, if $S = \{x_0, x_1\}$ and if T_x is a smooth metric, then $\mathrm{MedAxis}(S)$ is a smooth mediatrix hyper surface of dimension $d-1$ between the two points. In the Euclidean case, $T_x = \mathrm{Id}_d$, it corresponds to the separating affine hyperplane.

As detailed in Section 4.1.1, for a 2D manifold and a generic dense enough configuration of points, it is the union of portion of mediatrices between pairs of points, and triple points that are equidistant from three different points of S.

Section 2.6.2 explains how to compute numerically the medial axis.

Shape skeleton. The definition (1.20) of $\mathrm{MedAxis}(S)$ still holds when S is not a discrete set of points. The special case considered in Section 1.3.2 where Ω is a compact subset of $\mathbb{R}^d$ and $S = \partial\Omega$ is of particular importance for shape and surface modeling. In this setting, $\mathrm{MedAxis}(S)$ is often called the skeleton of the shape S, and is an important perceptual feature used to solve many computer vision problems. It has been studied extensively in computer vision as a basic tool for shape retrieval, see for instance [252]. One of the main issues is that the skeleton is very sensitive to local modifications of the shape, and tends to be complicated for non-smooth shapes.

Section 2.6.2 details how to compute and regularize numerically the skeleton of a shape. Figure 1.9 shows an example of skeleton for a 2D shape.

1.5 Geodesic Distance and Geodesic Curves

1.5.1 Geodesic Distance Map

The geodesic distance between two points defined in (1.15) can be generalized to the distance from a point x to a set of points $S \subset \Omega$ by computing the distance from x to its closest point in Ω, which defines the distance map

$$U_S(x) = \min_{y \in S} d(x, y). \tag{1.22}$$

Similarly a geodesic curve $\gamma^\star$ between a point $x \in \Omega$ and S is a curve $\gamma^\star \in \mathcal{P}(x, y)$ for some $y \in S$ such that $L(\gamma^\star) = U_S(x)$.

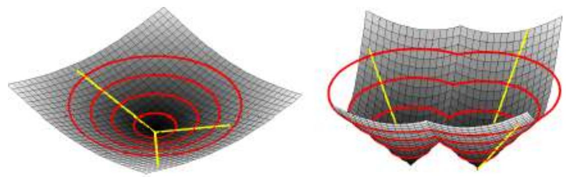

Fig. 1.10 Examples of geodesic distances and curves for a Euclidean metric with different starting configurations. Geodesic distance is displayed as an elevation map over $\Omega = [0,1]^2$. Red curves correspond to iso-geodesic distance lines, while yellow curves are examples of geodesic curves.

Figure 1.8, bottom row, shows examples of geodesic distance map to a single starting point $S = \{x_s\}$.

Figure 1.10 is a three-dimensional illustration of distance maps for a Euclidean metric in $\mathbb{R}^2$ from one (left) or two (right) starting points.

1.5.2 Eikonal Equation

For points x outside both the medial axis $\mathrm{MedAxis}(S)$ defined in (1.20) and S, one can prove that the geodesic distance map U_S is differentiable, and that it satisfies the following non-linear partial differential equation

$$\|\nabla U_S(x)\|_{T_x^{-1}} = 1, \text{ with boundary conditions } U_S(x) = 0 \text{ on } S, \quad (1.23)$$

where ∇U_S is the gradient vector of partial differentials in $\mathbb{R}^d$.

Unfortunately, even for a smooth metric T_x and simple set S, the medial axis $\mathrm{MedAxis}(S)$ is non-empty (see Figure 1.10, right, where the geodesic distance is clearly not differentiable at points equidistant from the starting points). To define U_S as a solution of a PDE even at points where it is not differentiable, one has to resort to a notion of weak solution. For a non-linear PDE such as (1.23), the correct notion of weak solution is the notion of viscosity solution, developed by Crandall and Lions [82, 83, 84].

A continuous function u is a viscosity solution of the Eikonal equation (1.23) if and only if for any continuously differentiable mapping $\varphi \in \mathrm{C}^1(\Omega)$ and for all $x_0 \in \Omega \backslash S$ local minimum of $u - \varphi$ we have

$$\|\nabla \varphi(x_0)\|_{T_{x_0}^{-1}} = 1$$

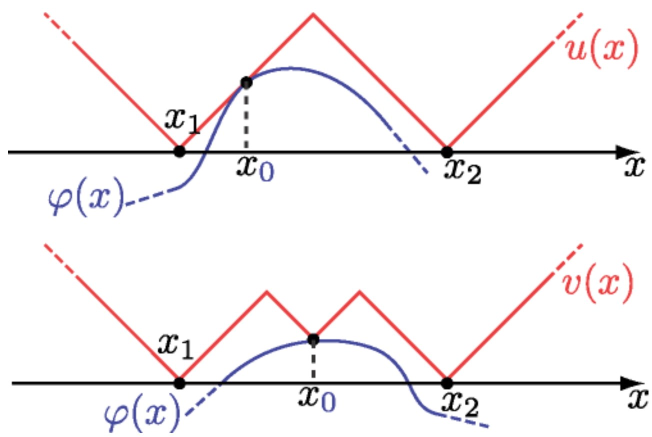

Fig. 1.11 Schematic view in 1D of the viscosity solution constrain.

For instance in 1D, $d = 1$, $\Omega = \mathbb{R}$, the distance function

$$u(x) = U_S(x) = \min(|x - x_1|, |x - x_2|)$$

from two points $S = \{x_1, x_2\}$ satisfies $|u'| = 1$ wherever it is differentiable. However, many other functions satisfies the same property, for example v, as shown on Figure 1.11. Figure 1.11, top, shows a $\mathrm{C}^1(\mathbb{R})$ function φ that reaches a local minimum for $u - \varphi$ at x_0. In this case, the equality $|\varphi'(x_0)| = 1$ holds. This condition would not be verified by v at point x_0. An intuitive vision of the definition of viscosity solution is that it prevents appearance of such inverted peaks outside S.

An important result from the viscosity solution of Hamilton–Jacobi equation, proved in [82, 83, 84], is that if S is a compact set, if $x \mapsto T_x$ is a continuous mapping, then the geodesic distance map U_S defined in (1.22) is the unique viscosity solution of the following Eikonal equation

$$\begin{cases} \forall x \in \Omega, & \|\nabla U_S(x)\|_{T_x^{-1}} = 1, \\ \forall x \in S, & U_S(x) = 0. \end{cases} \tag{1.24}$$

In the special case of an isotropic metric $T_x = W(x)^2 \mathrm{Id}_d$, one recovers the classical Eikonal equation

$$\forall x \in \Omega, \quad \|\nabla U_S(x)\| = W(x). \tag{1.25}$$

For the Euclidean case, $W(x) = 1$, one has $\|\nabla U_S(x)\| = 1$, whose viscosity solution for $S = \{x_s\}$ is $U_{x_s}(x) = \|x - x_s\|$.

1.5.3 Geodesic Curves

If the geodesic distance U_S is known, for instance by solving the Eikonal equation, a geodesic $\gamma^\star$ between some end point x_e and S is computed by gradient descent. This means that $\gamma^\star$ is the solution of the following ordinary differential equation

$$\begin{cases} \forall\, t > 0, \quad \dfrac{\mathrm{d}\gamma^\star(t)}{\mathrm{d}t} = -\eta_t v(\gamma^\star(t)), \\ \gamma^\star(0) = x_e. \end{cases} \tag{1.26}$$

where the tangent vector to the curve is the gradient of the distance, twisted by T_x^{-1}

$$v(x) = T_x^{-1} \nabla U_S(x),$$

and where $\eta_t > 0$ is a scalar function that controls the speed of the geodesic parameterization. To obtain a unit speed parameterization, $\|(\gamma^\star)'(t)\| = 1$, one needs to use

$$\eta_t = \|v(\gamma^\star(t))\|^{-1}.$$

If x_e is not on the medial axis $\mathrm{MedAxis}(S)$, the solution of (1.26) will not cross the medial axis for $t > 0$, so its solution is well defined for $0 \leq t \leq t_{x_e}$, for some t_{x_e} such that $\gamma^\star(t_{x_e}) \in S$.

For an isotropic metric $T_x = W(x)^2 \mathrm{Id}_d$, one recovers the gradient descent of the distance map proposed in [74]

$$\forall\, t > 0, \quad \frac{\mathrm{d}\gamma^\star(t)}{\mathrm{d}t} = -\eta_t \nabla U_S(\gamma^\star(t)).$$

Figure 1.10 illustrates the case where $T_x = \mathrm{Id}_2$: geodesic curves are straight lines orthogonal to iso-geodesic distance curves, and correspond to greatest slopes curves, since the gradient of a function is always orthogonal to its level curves.

References

[1] P. Agarwal and S. Suri, "Surface approximation and geometric partitions," *SIAM Journal of Computing*, vol. 19, pp. 1016–1035, 1998.

[2] J. C. Aguilar and J. B. Goodman, "Anisotropic mesh refinement for finite element methods based on error reduction," *Journal of Computational and Applied Mathematics*, vol. 193, no. 2, pp. 497–515, 2006.

[3] V. Akman, *Unobstructed Shortest Paths in Polyhedral Environments*. Springer-Verlag New York, Inc., New York, NY, USA, 1987.

[4] F. Alauzet, "Size gradation control of anisotropic meshes," *Finite Elements in Analysis and Design*, vol. 46, pp. 181–202, July 2010.

[5] P. Alliez, M. Attene, C. Gotsman, and G. Ucelli, "Recent advances in remeshing of surfaces," in *Shape Analysis and Structuring*, pp. 53–82, Springer, 2008.

[6] P. Alliez, D. Cohen-Steiner, O. Devillers, B. Lévy, and M. Desbrun, "Anisotropic polygonal remeshing," *ACM Transactions on Graphics*, vol. 22, no. 3, pp. 485–493, 2003.

[7] P. Alliez, D. Cohen-Steiner, M. Yvinec, and M. Desbrun, "Variational tetrahedral meshing," *ACM Transactions on Graphics*, vol. 24, no. 3, pp. 617–625, July 2005.

[8] P. Alliez, E. Colin de Verdière, O. Devillers, and M. Isenburg, "Isotropic surface remeshing," in *Proceedings of the Shape Modeling International*, pp. 49–58, IEEE Computer Society, 2003.

[9] N. Amenta, M. W. Bern, and D. Eppstein, "The crust and the beta-skeleton: Combinatorial curve reconstruction," *Graphical Models and Image Processing*, vol. 60, no. 2, pp. 125–135, 1998.

[10] P. Arbelaez and L. D. Cohen, "Energy partitions and image segmentation," *Journal of Mathematical Imaging and Vision*, vol. 20, nos. 1–2, pp. 43–57, January–March 2004.

[11] R. Ardon and L. D. Cohen, "Fast constrained surface extraction by minimal paths," *International Journal of Computer Vision*, vol. 69, no. 1, pp. 127–136, 2006.

[12] R. Ardon, L. D. Cohen, and A. Yezzi, "A new implicit method for surface segmentation by minimal paths in 3D images," *Applied Mathematics and Optimization*, vol. 55, no. 2, pp. 127–144, March 2007.

[13] N. Aspert, D. Santa-Cruz, and T. Ebrahimi, "MESH: Measuring error between surfaces using the hausdorff distance," *Proceedings of IEEE International Conference on Multimedia and Expo 2002*, vol. I, pp. 705–708, 2002.

[14] I. Babuška and A. K. Aziz, "On the angle condition in the finite element method," *SIAM Journal on Numerical Analysis*, vol. 13, no. 2, pp. 214–226, April 1976.

[15] F. A. Baqai, J. H. Lee, A. U. Agar, and J. P. Allebach, "Digital color halftoning," *IEEE Signal Processing Magazine*, vol. 22, no. 1, pp. 87–96, January 2005.

[16] P. J. Basser, J. Mattiello, and D. LeBihan, "Estimation of the effective self-diffusion tensor from the nmr spin echo," *Journal of Magnetic Resonance B*, vol. 103, no. 3, pp. 247–254, 1994.

[17] P. J. Basser, J. Mattiello, and D. Lebihan, "MR diffusion tensor spectroscopy and imaging," *Biophysical Journal*, vol. 66, pp. 259–267, 1994.

[18] P. N. Belhumeur, D. J. Kriegman, and A. L. Yuille, "The bas-relief ambiguity," *International Journal of Computer Vision*, vol. 35, no. 1, pp. 33–44, November 1999.

[19] M. Belkin and P. Niyogi, "Laplacian eigenmaps for dimensionality reduction and data representation," *Neural Computation*, vol. 15, no. 6, pp. 1373–1396, 2003.

[20] S. Belongie, J. Malik, and J. Puzicha, "Shape matching and object recognition using shape contexts," *IEEE Transactions on Pattern Analysis and Machine Intelligence*, vol. 24, no. 4, pp. 509–522, 2002.

[21] A. Ben Hamza and H. Krim, "Geodesic matching of triangulated surfaces," *IEEE Transactions on Image Processing*, vol. 15, no. 8, pp. 2249–2258, August 2006.

[22] F. Benmansour, G. Carlier, G. Peyré, and F. Santambrogio, "Numerical approximation of continuous traffic congestion equilibria," *Networks and Heterogeneous Media*, vol. 4, no. 3, pp. 605–623, 2009.

[23] F. Benmansour and L. D. Cohen, "Tubular structure segmentation based on minimal path method and anisotropic enhancement," *International Journal of Computer Vision*, to appear, 2010.

[24] F. Benmansour and L. D. Cohen, "Fast object segmentation by growing minimal paths from a single point on 2D or 3D images," *Journal of Mathematical Imaging and Vision*, vol. 33, no. 2, pp. 209–221, February 2009.

[25] M. Bern and D. Eppstein, "Mesh generation and optimal triangulation," in *Computing in Euclidean Geometry*, (F. K. Hwang and D. Z. Du, eds.), World Scientific, March 1992.

[26] M. Bernstein, V. de Silva, J. C. Langford, and J. B. Tenenbaum, "Graph approximations to geodesics on embedded manifolds," Standford Technical Report, 2005.

[27] P. J. Besl and N. D. McKay, "A method for registration of 3-d shapes," *IEEE Transactions on Pattern Analysis and Machine Intelligence*, vol. 14, no. 2, pp. 239–256, 1992.

[28] S. Beucher, "Watersheds of functions and picture segmentation," in *IEEE International Conference on Acoustics, Speech and Signal Processing*, pp. 1928–1931, Paris, 1982.

[29] S. Beucher and C. Lantuejoul, "On the use of the geodesic metric in image analysis," *Journal of Microscopy*, vol. 121, pp. 39–49, January 1981.

[30] S. Beucher and C. Lantuejoul, "Geodesic distance and image analysis," in *5th International Congress for Stereology, Salzburg, Austria*, pp. 138–142, 1979.

[31] T. N. Bishop, K. P. Bube, R. T. Cutler, R. T. Langan, P. L. Love, J. R. Resnick, R. T. Shuey, D. A. Spindler, and H. W. Wyld, "Tomographic determination of velocity and depth in laterally varying media," *Geophysics*, vol. 50, no. 6, pp. 903–923, 1985.

[32] J.-D. Boissonnat, C. Wormser, and M. Yvinec, "Anisotropic diagrams: Labelle shewchuk approach revisited," *Theoretical Computer Science*, vol. 408, nos. 2–3, pp. 163–173, 2008.

[33] J.-D. Boissonnat, C. Wormser, and M. Yvinec, "Locally uniform anisotropic meshing," in *Proceedings of SCG'08*, pp. 270–277, New York, NY, USA: ACM, 2008.

[34] I. Borg and P. Groenen, *Modern Multidimensional Scaling.* Springer-Verlag, New York, 1997. Theory and applications.

[35] F. Bornemann and C. Rasch, "Finite-element discretization of static hamilton-jacobi equations based on a local variational principle," *Computing and Visualization in Science*, vol. 9, no. 2, pp. 57–69, 2006.

[36] H. Borouchaki, P. L. George, and B. Mohammadi, "Delaunay mesh generation governed by metric specifications. Part I. algorithms," *Finite Elements in Analysis and Design*, vol. 25, nos. 1–2, pp. 61–83, 1997.

[37] H. Borouchaki, F. Hecht, and P. J. Frey, "Mesh gradation control," *International Journal for Numerical Methods in Engineering*, vol. 43, no. 6, pp. 1143–1165, 1998.

[38] F. J. Bossen and P. S. Heckbert, "A pliant method for anisotropic mesh generation," in *5th International Meshing Roundtable*, pp. 63–74, October 1996.

[39] S. Bougleux, G. Peyré, and L. Cohen, "Image compression with geodesic anisotropic triangulations," in *Proceedings of ICCV'09*, 2009.

[40] S. Bougleux, G. Peyré, and L. D. Cohen, "Anisotropic geodesics for perceptual grouping and domain meshing," in *Proceedings of ECCV'08*, vol. 5303 of *Lecture Notes in Computer Science*, (D. A. Forsyth, P. H. S. Torr, and A. Zisserman, eds.), pp. 129–142, Springer, 2008.

[41] Y. Boykov and V. Kolmogorov, "Computing geodesics and minimal surfaces via graph cuts," in *Proceedings of ICCV'03*, pp. 26–33, IEEE Computer Society, 2003.

[42] A. Bronstein, M. Bronstein, and R. Kimmel, *Numerical Geometry of Non-Rigid Shapes*. Springer, 2007.

[43] A. M. Bronstein, M. M. Bronstein, A. M. Bruckstein, and R. Kimmel, "Analysis of two-dimensional non-rigid shapes," *International Journal of Computer Vision*, vol. 78, no. 1, pp. 67–88, June 2008.

[44] A. M. Bronstein, M. M. Bronstein, A. M. Bruckstein, and R. Kimmel, "Partial similarity of objects, or how to compare a centaur to a horse," *International Journal of Computer Vision*, vol. 84, no. 2, pp. 163–183, 2009.

[45] A. M. Bronstein, M. M. Bronstein, and R. Kimmel, "Efficient computation of isometry-invariant distances between surfaces," *SIAM Journal on Scientific Computing*, vol. 28, no. 5, pp. 1812–1836, 2006.

[46] A. M. Bronstein, M. M. Bronstein, and R. Kimmel, "Calculus of nonrigid surfaces for geometry and texture manipulation," *IEEE Transactions on Visualization and Computer Graphics*, vol. 13, no. 5, pp. 902–913, 2007.

[47] A. M. Bronstein, M. M. Bronstein, and R. Kimmel, "Expression-invariant representations of faces," *IEEE Transactions on Image Processing*, vol. 16, no. 1, pp. 188–197, January 2007.

[48] A. M. Bronstein, M. M. Bronstein, and R. Kimmel, "Weighted distance maps computation on parametric three-dimensional manifolds," *Journal of Computational Physics*, vol. 225, no. 1, pp. 771–784, 2007.

[49] A. M. Bronstein, M. M. Bronstein, R. Kimmel, M. Mahmoudi, and G. Sapiro, "A Gromov–Hausdorff framework with diffusion geometry for topologically-robust non-rigid shape matching," *International Journal of Computer Vision*, vol. 89, no. 3, pp. 266–286, 2010.

[50] A. M. Bronstein, M. M. Bronstein, M. Ovsjanikov, and L. J. Guibas, "Shape google: Geometric words and expressions for invariant shape retrieval," *ACM Transactions on Graphics*, 2010.

[51] M. M. Bronstein, A. M. Bronstein, and R. Kimmel, "Generalized multidimensional scaling: A framework for isometry-invariant partial surface matching," *Proceedings of the National Academy of Sciences*, vol. 103, no. 5, pp. 1168–1172, 2006.

[52] M. M. Bronstein, A. M. Bronstein, R. Kimmel, and I. Yavneh, "Multigrid multidimensional scaling," *Numerical Linear Algebra with Applications*, vol. 13, nos. 2–3, pp. 149–171, 2006.

[53] D. Burago, Y. Burago, and S. Ivanov, *A Course in Metric Geometry*, vol. 33. Springer-Verlag, 2001.

[54] B. Bustos, D. A. Keim, D. Saupe, T. Schreck, and D. V. Vranić, "Feature-based similarity search in 3D object databases," *ACM Computing Surveys*, vol. 37, no. 4, pp. 345–387, 2005.

[55] G. J. Butler, "Simultaneous packing and covering in euclidean space," in *Proceedings of the London Mathematical Society*, vol. 25, pp. 721–735, June 1972.

[56] G. Buttazzo, A. Davini, I. Fragal, and F. Maciá, "Optimal riemannian distances preventing mass tranfer," *The Journal für die Reine and Angewandte Mathematic*, vol. 575, pp. 157–171, 2004.

[57] J. Canny, "A computational approach to edge detection," *IEEE Transactions Pattern Analysis and Machine Intelligence*, vol. 8, no. 6, pp. 679–698, November 1986.

[58] G. Carlier, C. Jimenez, and F. Santambrogio, "Optimal transportation with traffic congestion and wardrop equilibria," *SIAM Journal on Control and Optimization*, vol. 47, no. 3, pp. 1330–1350, 2008.

[59] V. Caselles, F. Catté, T. Coll, and F. Dibos, "A geometric model for active contours in image processing," *Numerische Mathematik*, vol. 66, no. 1, pp. 1–31, 1993.

[60] V. Caselles, R. Kimmel, and G. Sapiro, "Geodesic active contours," *International Journal of Computer Vision*, vol. 22, no. 1, pp. 61–79, 1997.

[61] J. Chen and Y. Hahn, "Shortest path on a polyhedron," in *Proceedings of Sixth ACM Symposium on Computational Geometry*, pp. 360–369, 1990.

[62] Y. Chen and G. Medioni, "Object modelling by registration of multiple range images," *International Journal of Image and Vision Computing*, vol. 10, no. 3, pp. 145–155, April 1992.

[63] L. P. Chew, "Constrained Delaunay triangulations," *Algorithmica*, vol. 4, pp. 97–108, 1989.

[64] L. P. Chew, "Guaranteed-quality triangular meshes," Technical Report TR-89-983, Department of Computer Science, Cornell University, 1989.

[65] L. P. Chew, "Guaranteed-quality mesh generation for curved surfaces," in *Proceedings of SCG '93*, pp. 274–280, New York, NY, USA: ACM, 1993.

[66] D. L. Chopp, "Some improvements of the fast marching method," *SIAM Journal on Scientific Computing*, vol. 23, no. 1, pp. 230–244, 2001.

[67] P. Cignoni, C. Rocchini, and R. Scopigno, "Metro: Measuring error on simplified surfaces," *Computer Graphics Forum*, vol. 17, no. 2, pp. 167–174, 1998.

[68] U. Clarenz, M. Rumpf, and A. Telea, "Robust feature detection and local classification for surfaces based on moment analysis," *IEEE Transactions on Visualization and Computer Graphics*, vol. 10, no. 5, pp. 516–524, 2004.

[69] K. L. Clarkson, "Building triangulations using epsilon-nets," in *Proceedings of STOC*, (J. M. Kleinberg, ed.), pp. 326–335, ACM, 2006.

[70] L. D. Cohen, "On active contour models and balloons," *CVGIP: Image Understanding*, vol. 53, no. 2, pp. 211–218, 1991.

[71] L. D. Cohen, "Multiple contour finding and perceptual grouping using minimal paths," *Journal of Mathematical Imaging and Vision*, vol. 14, no. 3, pp. 225–236, May 2001.

[72] L. D. Cohen, "Minimal paths and fast marching methods for image analysis," in *Handbook of Mathematical Methods in Computer Vision*, (N. Paragios, Y. Chen, and O. Faugeras, eds.), Springer, 2005.

[73] L. D. Cohen and I. Cohen, "Finite element methods for active contour models and balloons for 2-D and 3-D images," *IEEE Transactions on Pattern Analysis and Machine Intelligence*, p. 15, 1993.

[74] L. D. Cohen and R. Kimmel, "Global minimum for active contour models: A minimal path approach," *International Journal of Computer Vision*, vol. 24, no. 1, pp. 57–78, August 1997.

[75] L. Cohen and R. Kimmel, "Regularization properties for minimal geodesics of a potential energy," in *ICAOS*, 1996.

[76] L. D. Cohen, "A new approach of vector quantization for image data compression and texture detection," in *International Conference on Pattern Recognition, ICPR'88*, Rome, 1988.

[77] L. D. Cohen and T. Deschamps, "Grouping connected components using minimal path techniques," in *Proceedings of IEEE CVPR'01*, Kauai, Hawai, December 2001.

[78] L. D. Cohen and T. Deschamps, "Multiple contour finding and perceptual grouping as a set of energy minimizing paths," in *Proceedings of Third International Workshop on Energy Minimization Methods in Computer Vision and Pattern Recognition (EMMCVPR — 2001)*, Springer, 2001.

[79] L. D. Cohen and T. Deschamps, "Segmentation of 3D tubular objects with adaptive front propagation and minimal tree extraction for 3D medical imaging," *Computer Methods in Biomechanics and Biomedical Engineering*, vol. 10, no. 4, pp. 289–305, August 2007.

[80] D. Cohen-Steiner and J.-M. Morvan, "Second fundamental measure of geometric sets and local approximation of curvatures," *Journal of Differential Geometry*, vol. 74, no. 3, pp. 363–394, 2006.

[81] J. H. Conway and N. J. A. Sloane, *Sphere Packings, Lattices and Groups*. New York, NY, USA: Springer-Verlag, 2nd Edition, 1993.

[82] M. G. Crandall, H. Ishii, and P. L. Lions, "User's guide to viscosity solutions of second order partial differential equations," *Bulletin of the American Mathematical Society*, vol. 27, no. 1, pp. 1–67, 1992.

[83] M. G. Crandall and P. L. Lions, "Viscosity solutions of Hamilton–Jacobi equations," *Transactions of the American Mathematical Society*, vol. 277, no. 1, pp. 1–42, 1983.

[84] M. G. Crandall and P.-L. Lions, "Two approximations of solutions of Hamilton–Jacobi equations," *Mathematics of Computation*, vol. 43, no. 167, pp. 1–19, 1984.

[85] O. Cuisenaire, "Distance transformations: Fast algorithms and applications to medical image processing," PhD thesis, Université Catholique de Louvain, Louvain-La-Neuve, Belgique, 1999.

[86] O. Cuisenaire and B. Macq, "Fast and exact signed Euclidean distance transformation with linear complexity," in *IEEE International Conference on Acoustics, Speech and Signal Processing (ICASSP'99)*, Lecture Notes in Computer Science, pp. 3293–3296, IEEE, 1999.

[87] O. Cuisenaire and B. Macq, "Fast euclidean distance transformation by propagation using multiple neighborhoods," *Computer Vision and Image Understanding*, vol. 76, no. 2, pp. 163–172, 1999.

[88] P.-E. Danielsson, "Euclidean distance mapping," *Computer Graphics and Image Processing*, vol. 14, pp. 227–248, 1980.

[89] S. Dasgupta and P. M. Long, "Performance guarantees for hierarchical clustering," *Journal of Computer and System Sciences*, vol. 70, no. 4, pp. 555–569, 2005.

[90] M. de Berg, M. van Kreveld, M. Overmars, and O. Schwarzkopf, *Computational Geometry: Algorithms and Applications*. Springer-Verlag, 2nd Edition, 2000.

[91] J. de Leeuw, "Applications of convex analysis to multidimensional scaling," in *Recent Developments in Statistics*, (F. Brodeau and G. Romie et al., eds.), pp. 133–145, Barra, 1977.

[92] V. de Silva and J. B. Tenenbaum, “Sparse multidimensional scaling using landmark points,” Technical Report, Stanford University, 2004.
[93] B. Delaunay, “Sur la sphère vide,” *Izvestia Akademii Nauk SSSR, Otdelenie Matematicheskikh i Estestvennykh Nauk*, vol. 7, pp. 793–800, 1934.
[94] L. Demaret, N. Dyn, and A. Iske, “Image compression by linear splines over adaptive triangulations,” *Signal Processing*, vol. 86, no. 7, pp. 1604–1616, 2006.
[95] T. Deschamps and L. D. Cohen, “Minimal paths in 3D images and application to virtual endoscopy,” in *Proceedings of sixth European Conference on Computer Vision (ECCV'00)*, Dublin, Ireland, 26th June–1st July 2000.
[96] T. Deschamps and L. D. Cohen, “Fast extraction of minimal paths in 3D images and applications to virtual endoscopy,” *Medical Image Analysis*, vol. 5, no. 4, pp. 281–299, December 2001.
[97] T. Deschamps and L. D. Cohen, “Fast extraction of tubular and tree 3D surfaces with front propagation methods,” in *Proceedings of 16th IEEE International Conference on Pattern Recognition (ICPR'02)*, pp. 731–734, August: Quebec, Canada, 2002.
[98] T. Deschamps and L. D. Cohen, “Grouping connected components using minimal path techniques,” in *Geometrical Method in Biomedical Image Processing*, (R. Malladi, ed.), Springer, 2002.
[99] A. Desolneux, L. Moisan, and J.-M. Morel, “A grouping principle and four applications,” *IEEE Transactions on Pattern Analysis and Machine Intelligence*, vol. 25, no. 4, pp. 508–513, 2003.
[100] Y. Devir, G. Rosman, A. M. Bronstein, M. M. Bronstein, and R. Kimmel, “On reconstruction of non-rigid shapes with intrinsic regularization,” in *Proceedings of Workshop on Nonrigid Shape Analysis and Deformable Image Alignment (NORDIA)*, 2009.
[101] T. K. Dey, *Curve and Surface Reconstruction: Algorithms with Mathematical Analysis*. Cambridge University Press, 2007.
[102] T. K. Dey and P. Kumar, “A simple provable algorithm for curve reconstruction,” in *Proceedings of SODA'99*, pp. 893–894, 1999.
[103] E. W. Dijkstra, “A note on two problems in connexion with graphs,” *Numerische Mathematik*, vol. 1, no. 1, pp. 269–271, December 1959.
[104] D. L. Donoho and C. Grimes, “Hessian eigenmaps: Locally linear embedding techniques for high-dimensional data,” *Proceedings of the National Academy of Sciences*, vol. 100, no. 10, pp. 5591–5596, 2003.
[105] D. L. Donoho and C. Grimes, “Image manifolds which are isometric to euclidean space,” *Journal of Mathematical Imaging and Vision*, vol. 23, no. 1, pp. 5–24, July 2005.
[106] J. Doran, “An approach to automatic problem-solving,” *Machine Intelligence*, vol. 1, pp. 105–127, 1967.
[107] Q. Du and M. Emelianenko, “Acceleration schemes for computing centroidal Voronoi tessellations,” *Numerical Linear Algebra with Applications*, vol. 13, nos. 2–3, pp. 173–192, 2006.
[108] Q. Du, M. Emelianenko, and L. Ju, “Convergence of the lloyd algorithm for computing centroidal voronoi tessellations,” *SIAM Journal on Numerical Analysis*, vol. 44, pp. 102–119, 2006.

[109] Q. Du, V. Faber, and M. Gunzburger, “Centroidal Voronoi tessellations: Applications and algorithms,” *SIAM Review*, vol. 41, pp. 637–676, 1999.

[110] Q. Du and M. Gunzburger, “Grid generation and optimization based on centroidal Voronoi tessellations,” *Applied Mathematics and Computation*, vol. 133, nos. 2–3, pp. 591–607, December 2002.

[111] Q. Du and D. Wang, “Anisotropic centroidal Voronoi tessellations and their applications,” *SIAM Journal on Scientific Computing*, vol. 26, no. 3, pp. 737–761, May 2005.

[112] N. Dyn, D. Levin, and S. Rippa, “Data dependent triangulations for piecewise linear interpolation,” *IMA Journal of Numerical Analysis*, vol. 10, no. 1, pp. 137–154, January 1990.

[113] A. Elad (Elbaz) and R. Kimmel, “On bending invariant signatures for surfaces,” *IEEE Transactions on Pattern Analysis and Machine Intelligence*, vol. 25, no. 10, pp. 1285–1295, 2003.

[114] Y. Eldar, M. Lindenbaum, M. Porat, and Y. Y. Zeevi, “The farthest point strategy for progressive image sampling,” *IEEE Transactions on Image Processing*, vol. 6, no. 9, pp. 1305–1315, September 1997.

[115] R. Fabbri, L. Costa, J. Torelli, and O. Bruno, “2D euclidean distance transform algorithms: A comparative survey,” *ACM Computing Surveys*, vol. 40, no. 1, pp. 1–44, 2008.

[116] Z. Feng, I. Hotz, B. Hamann, and K. I. Joy, “Anisotropic noise samples,” *IEEE Transactions on Visualization and Computer Graphics*, vol. 14, no. 2, pp. 342–354, 2008.

[117] D. J. Field, A. Hayes, and R. F. Hess, “Links contour integration by the human visual system: Evidence for a local ‘association field’,” *Vision Research*, vol. 33, no. 2, pp. 173–193, January 1993.

[118] M. S. Floater and K. Hormann, “Surface parameterization: A tutorial and survey,” in *Advances in Multiresolution for Geometric Modelling*, (N. A. Dodgson, M. S. Floater, and M. A. Sabin, eds.), pp. 157–186, Springer Verlag, 2005.

[119] R. W. Floyd and L. Steinberg, “An adaptive algorithm for spatial greyscale,” *Proceedings of the Society for Information Display*, vol. 17, no. 2, pp. 75–77, 1976.

[120] R. Floyd, “Algorithm 245: Treesort,” *Communications of the ACM*, vol. 7, no. 12, p. 701, 1964.

[121] S. Fomel, “A variational formulation of the fast marching eikonal solver,” Stanford Technology Report 95, Stanford Exploration Project, pp. 127–149, 1997.

[122] M. Frenkel and R. Basri, “Curve matching using the fast marching method,” in *Proceedings of EMMCVPR*, (A. Rangarajan, ed.), pp. 35–51, 2003.

[123] M. Garland and P. Heckbert, “Surface simplification using quadric error metrics,” in *Proceedings of SIGGRAPH 1997*, pp. 209–215, 1997.

[124] P. L. George, H. Borouchaki, P. J. Frey, P. Laug, and E. Saltel, “Mesh generation and mesh adaptivity: Theory, techniques,” in *Encyclopedia of Computational Mechanics*, (E. Stein, R. de Borst, and T. J. R. Hughes, eds.), John Wiley and Sons Ltd., 2004.

[125] A. V. Goldberg and C. Harrelson, “Computing the shortest path: A search meets graph theory,” in *Proceedings of SODA*, pp. 156–165, SIAM, 2005.

[126] T. F. Gonzalez, "Clustering to minimize the maximum intercluster distance," *Theoretical Computer Science*, vol. 38, nos. 2–3, pp. 293–306, June 1985.

[127] L. Gorelick, M. Galun, E. Sharon, R. Basri, and A. Brandt, "Shape representation and classification using the poisson equation," *IEEE Transactions on Pattern Analysis and Machine Intelligence*, vol. 28, no. 12, pp. 1991–2005, December 2006.

[128] M. Gromov, *Metric Structures for Riemannian and Non-Riemannian Spaces*. Birkhauser Boston, 1999.

[129] P. M. Gruber, "Asymptotic estimates for best and stepwise approximation of convex bodies. I," *Forum Mathematicum*, vol. 5, pp. 281–297, 1993.

[130] P. M. Gruber, "Optimum quantization and its applications," *Advances in Mathematics*, vol. 186, pp. 456–497, 2004.

[131] G. Guy and G. Medioni, "Inferring global perceptual contours from local features," *International Journal of Computer Vision*, vol. 20, nos. 1–2, pp. 113–133, 1996.

[132] P. Hart, N. Nilsson, and B. Raphael, "A formal basis for the heuristic determination of minimum-cost paths," *IEEE Transactions on Systems Science and Cybernetics*, vol. SSC-4, no. 2, pp. 100–107, July 1968.

[133] M. S. Hassouna and A. A. Farag, "Robust skeletonization using the fast marching method," in ICIP05, vol. I, pp. 437–440, 2005.

[134] H. Hopf and W. Rinow, "Ueber den begriff der vollstandigen differentialgeometrischen flachen," *Commentarii Mathematici Helvetici*, vol. 3, pp. 209–225, 1931.

[135] H. Hoppe, "Progressive meshes," in *Proceedings of SIGGRAPH 1996*, pp. 99–108, 1996.

[136] B. K. P. Horn, "Obtaining shape from shading information," in *The Psychology of Computer Vision*, pp. 115–155, 1975.

[137] A. Ion, N. Artner, G. Peyré, S. B. López Mármol, W. G. Kropatsch, and L. Cohen, "3D shape matching by geodesic eccentricity," in *Proceedings of Workshop on Search in 3D*, Anchorage, Alaska: IEEE, June 2008.

[138] A. Ion, G. Peyré, Y. Haxhimusa, S. Peltier, W. G. Kropatsch, and L. Cohen, "Shape matching using the geodesic eccentricity transform — a study," in *The 31st Annual Workshop of the Austrian Association for Pattern Recognition (OAGM/AAPR)*, (C. Beleznai, W. Ponweiser, and M. Vincze, eds.), pp. 97–104, Schloss Krumbach, Austria: OCG, May 2007.

[139] A. K. Jain, M. N. Murty, and P. J. Flynn, "Data clustering: A review," *ACM Computing Surveys*, vol. 31, no. 3, pp. 264–323, 1999.

[140] S. Jbabdi, P. Bellec, R. Toro, J. Daunizeau, M. Pélégrini-Issac, and H. Benali, "Accurate anisotropic fast marching for diffusion-based geodesic tractography," *Journal of Biomedical Imaging*, vol. 2008, no. 1, pp. 1–12, 2008.

[141] W.-K. Jeong and R. T. Whitaker, "A fast iterative method for eikonal equations," *SIAM Journal on Scientific Computing*, vol. 30, no. 5, pp. 2512–2534, 2008.

[142] A. E. Johnson and M. Hebert, "Using spin images for efficient object recognition in cluttered 3D scenes," *IEEE Transactions on Pattern Analysis and Machine Intelligence*, vol. 21, no. 5, pp. 433–449, 1999.

[143] H. Karcher, “Riemannian center of mass and mollifier smoothing,” *Communications on Pure and Applied Mathematics*, vol. 5, no. 30, pp. 509–541, 1977.

[144] M. Kass, A. Witkin, and D. Terzopoulos, “Snakes: Active contour models,” *International Journal of Computer Vision*, vol. 1, no. 4, pp. 321–331, January 1988.

[145] S. Kim, “An ≀(\) level set method for eikonal equations,” *SIAM Journal on Scientific Computing*, vol. 22, no. 6, pp. 2178–2193, 2001.

[146] B. B. Kimia, A. R. Tannenbaum, and S. W. Zucker, “Shapes, shocks, and deformations I: The components of two-dimensional shape and the reaction-diffusion space,” *International Journal of Computer Vision*, vol. 15, no. 3, pp. 189–224, 1995.

[147] R. Kimmel, *Numerical Geometry of Images: Theory, Algorithms, and Applications*. Springer, 2004.

[148] R. Kimmel, A. Amir, and A. M. Bruckstein, “Finding shortest paths on surfaces using level sets propagation,” *IEEE Transactions on Pattern Analysis and Machine Intelligence*, vol. 17, no. 6, pp. 635–640, 1995.

[149] R. Kimmel and A. M. Bruckstein, “Shape offsets via level sets,” *Computer Aided Design*, vol. 25, pp. 154–162, 1993.

[150] R. Kimmel and N. Kiryati, “Finding the shortest paths on surfaces by fast global approximation and precise local refinement,” *International Journal of Pattern Recognition and Artificial Intelligence*, vol. 10, no. 6, pp. 643–656, 1996.

[151] R. Kimmel and J. A. Sethian, “Computing geodesic paths on manifolds,” *Proceedings of the National Academy of Sciences*, vol. 95, no. 15, pp. 8431–8435, 1998.

[152] R. Kimmel and J. A. Sethian, “Fast marching methods on triangulated domains,” *Proceedings of the National Academy of Sciences*, vol. 95, no. 15, pp. 8431–8435, July 1998.

[153] R. Kimmel and J. A. Sethian, “Optimal algorithm for shape from shading and path planning,” *Journal of Mathematical Imaging and Vision*, vol. 14, p. 2001, 2001.

[154] E. Klassen, A. Srivastava, W. Mio, and S. H. Joshi, “Analysis of planar shapes using geodesic paths on shape spaces,” *IEEE Transactions on Pattern Analysis and Machine Intelligence*, vol. 26, no. 3, pp. 372–383, March 2004.

[155] E. Konukoglu, “Modeling glioma growth and personalizing growth models in medical images,” PhD thesis, University of Nice-Sophia Antipolis, 2009.

[156] U. Kothe, “Edge and junction detection with an improved structure tensor,” in *Proceedings of DAGM03*, pp. 25–32, 2003.

[157] J. B. Kruskal, “Multidimensional scaling by optimizing goodness of fit to a nonmetric hypothesis,” *Psychometrika*, vol. 29, pp. 1–27, 1964.

[158] F. Labelle and J. R. Shewchuk, “Anisotropic voronoi diagrams and guaranteed-quality anisotropic mesh generation,” in *Proceedings of SCG ’03*, pp. 191–200, New York: ACM Press, 2003.

[159] L. J. Latecki and R. Lakamper, “Shape similarity measure based on correspondence of visual parts,” *IEEE Transactions on Pattern Analysis and Machine Intelligence*, vol. 22, no. 10, pp. 1185–1190, October 2000.

[160] J.-C. Latombe, *Robot Motion Planning*. Norwell, MA, USA: Kluwer Academic Publishers, 1991.

[161] S. M. LaValle, *Planning Algorithms*. Cambridge, U.K.: Cambridge University Press, 2006.

[162] H. Le, "Locating Fréchet means with application to shape spaces," *Advances in Applied Probability*, vol. 33, pp. 324–338, 2001.

[163] H. Le and D. G. Kendall, "The riemannian structure of euclidean shape space: A novel environment for statistics," *Annals of Statistics*, vol. 21, pp. 1225–1271, 1993.

[164] J. M. Lee, *Riemannian Manifolds*. Springer-Verlag, 1980.

[165] G. Leibon and D. Letscher, "Delaunay triangulations and voronoi diagrams for riemannian manifolds," in *SCG '00: Proceedings of the Sixteenth Annual Symposium on Computational Geometry*, pp. 341–349, New York, NY, USA: ACM, 2000.

[166] M. Levoy, K. Pulli, S. Rusinkiewicz, D. Koller, L. Pereira, M. Ginzton, S. Anderson, J. Davis, J. Ginsberg, B. Curless, J. Shade, and D. Fulk, "The digital michelangelo project: 3D scanning of large statues," in *Proceedings of Siggraph 2000*, pp. 131–144, New York: ACM Press, 2000.

[167] F. Leymarie and M. D. Levine, "Simulating the grassfire transform using an active contour model," *IEEE Transactions on Pattern Analysis and Machine Intelligence*, vol. 14, no. 1, pp. 56–75, January 1992.

[168] H. Li and A. Yezzi, "Vessels as 4D curves: Global minimal 4D paths to extract 3D tubular surfaces and centerlines," *IEEE Transactions on Medical Imaging*, vol. 26, no. 9, pp. 1213–1223, 2007.

[169] H. Li, A. Yezzi, and L. D. Cohen, "3D multi-branch tubular surface and centerline extraction with 4d iterative key points," in *Proceedings of 12th International Conference on Medical Image Computing and Computer Assisted Intervention, MICCAI'09*, London, UK: Imperial College, 2009.

[170] X. Li, J.-F. Remacle, N. Chevaugeon, and M. S. Shephard, "Anisotropic mesh gradation control," in *Proceedings of 13th International Meshing Rountable*, pp. 401–412, 2004.

[171] S. X. Liao and M. Pawlak, "On image analysis by moments," *IEEE Transactions on Pattern Analysis and Machine Intelligence*, vol. 18, no. 3, pp. 254–266, 1996.

[172] S. Liapis, E. Sifakis, and G. Tziritas, "Color and/or texture segmentation using deterministic relaxation and fast marching algorithms," in *ICPR*, vol III, pp. 617–620, 2000.

[173] M. Lin and D. Manocha, "Collision and proximity queries," in *Handbook of Discrete and Computational Geometry*, 2003.

[174] H. Ling and D. W. Jacobs, "Shape classification using the inner-distance," *IEEE Transactions on Pattern Analysis and Machine Intelligence*, vol. 29, no. 2, pp. 286–299, 2007.

[175] P. L. Lions, E. Rouy, and A. Tourin, "Shape-from-shading, viscosity solutions and edges," *Numerische Mathematik*, vol. 64, no. 3, pp. 323–353, March 1993.

[176] Y. Liu, W. Wang, B. Lévy, F. Sun, D.-M. Yan, L. Lu, and C. Yang, "On centroidal voronoi tessellation — energy smoothness and fast computation," *ACM Transactions on Graphics*, vol. 28, no. 4, 2009.

[177] S. P. Lloyd, "Least squares quantization in PCM," *IEEE Transactions on Information Theory*, vol. 28, no. 2, pp. 129–136, 1982.

[178] R. Malladi and J. A. Sethian, "An $o(n\log(n))$ algorithm for shape modeling," *Proc. of the National Academy of Sciences*, vol. 93, pp. 9389–9392, 1996.

[179] R. Malladi, J. A. Sethian, and B. C. Vemuri, "Shape modeling with front propagation: A level set approach," *IEEE Transactions on Pattern Analysis and Machine Intelligence*, vol. 17, no. 2, pp. 158–175, 1995.

[180] S. Manay, D. Cremers, B. W. Hong, A. J. Yezzi, and S. Soatto, "Integral invariants for shape matching," *IEEE Transactions on Pattern Analysis and Machine Intelligence*, vol. 28, no. 10, pp. 1602–1618, October 2006.

[181] P. Matula, J. Huben, and M. Kozubek, "Fast marching 3D reconstruction of interphase chromosomes," in *ECCV Workshops CVAMIA and MMBIA,* vol. 3117 of *Lecture Notes in Computer Science*, (M. Sonka, I. A. Kakadiaris, and J. Kybic, eds.), pp. 385–394, Springer, 2004.

[182] C. R. Maurer, R. Qi, and V. Raghavan, "A linear time algorithm for computing exact Euclidean distance transforms of binary images in arbitrary dimensions," *IEEE Transactions on Pattern Analysis and Machine Intelligence*, vol. 25, no. 2, pp. 265–270, 2003.

[183] G. Medioni, M.-S. Lee, and C.-K. Tang, *A Computational Framework for Segmentation and Grouping*. Elsevier, 2000.

[184] A. Meijster, J. B. T. M. Roerdink, and W. H. Hesselink, "A general algorithm for computing distance transforms in linear time," in *Mathematical Morphology and Its Applications to Image and Signal Processing*, pp. 331–340, Kluwer, 2000.

[185] F. Memoli, "On the use of gromov-hausdorff distances for shape comparison," in *Proceedings of Symposium on Point Based Graphics 2007*, 2007.

[186] F. Mémoli, "Spectral Gromov–Wasserstein distances for shape matching," in *Workshop on Non-Rigid Shape Analysis and Deformable Image Alignment (ICCV workshop, NORDIA'09)*, October 2009.

[187] F. Memoli and G. Sapiro, "A theoretical and computational framework for isometry invariant recognition of point cloud data," *Foundations of Computational Mathematics*, vol. 5, no. 3, pp. 313–347, 2005.

[188] F. Meyer, "Topographic distance and watershed lines," *Signal Processing*, vol. 38, no. 1, pp. 113–125, July 1994.

[189] F. Meyer and P. Maragos, "Multiscale morphological segmentations based on watershed, flooding, and eikonal PDE," in *Scale Space*, pp. 351–362, 1999.

[190] J.-M. Mirebeau and A. Cohen, "Greedy bisection generates optimally adapted triangulations," Technical report, Laboratoire Jacques-Louis Lions, 2008.

[191] J. Mitchell, D. Mount, and C. Papadimitriou, "The discrete geodesic problem," *SIAM Journal on Computing*, vol. 16, no. 4, pp. 647–668, 1987.

[192] J. S. B. Mitchell and C. H. Papadimitriou, "The weighted region problem: Finding shortest paths through a weighted planar subdivision," *Journal of the ACM*, vol. 38, no. 1, pp. 18–73, 1991.

[193] F. Mokhtarian and A. K. Mackworth, "A theory of multiscale, curvature-based shape representation for planar curves," *IEEE Transactions on Pattern Analysis and Machine Intelligence*, vol. 14, no. 8, pp. 789–805, August 1992.

[194] U. Montanari, "A method for obtaining skeletons using a quasi-euclidean distance," *Journal of the ACM*, vol. 15, no. 4, pp. 600–624, 1968.

[195] D. Mumford, "Mathematical theories of shape: Do they model perception?," *Geometric Methods in Computer Vision*, vol. 1570, pp. 2–10, 1991.

[196] D. Mumford, "Elastica and computer vision," in *Algebraic Geometry and its Applications*, (C. L. Bajaj, ed.), pp. 491–506, 1994.

[197] D. Mumford and J. Shah, "Optimal approximations by piecewise smooth functions and associated variational problems," *Communications on Pure and Applied Mathematics*, vol. XLII, no. 4, 1989.

[198] L. Najman and M. Schmitt, "Geodesic saliency of watershed contours and hierarchical segmentation," *IEEE Transactions on Pattern Analysis and Machine Intelligence*, vol. 18, no. 12, pp. 1163–1173, 1996.

[199] M. Niemeijer, J. J. Staal, B. van Ginneken, M. Loog, and M. D. Abramoff, "Comparative study of retinal vessel segmentation methods on a new publicly available database," in *SPIE Medical Imaging,* vol. 5370, (J. M. Fitzpatrick and M. Sonka, eds.), pp. 648–656, SPIE, 2004.

[200] B. Nilsson and A. Heyden, "Segmentation of dense leukocyte clusters," in *Proceedings of MMBIA '01*, Washington, DC, USA: IEEE Computer Society, 2001.

[201] N. J. Nilsson, *Problem-solving Methods in Artificial Intelligence*. New York: McGraw-Hill, 1971.

[202] M. Novotni and R. Klein, "Computing geodesic distances on triangular meshes," in *Proceedings of WSCG'2002*, 2002.

[203] R. L. Ogniewicz, *Discrete Voronoi Skeleton*. Hartung-Gorre, 1993.

[204] Y. Ohtake, A. Belyaev, and H.-P. Seidel, "Ridge-valley lines on meshes via implicit surface fitting," *ACM Transactions on Graphics*, vol. 23, no. 3, pp. 609–612, 2004.

[205] K. Onishi and J. Itoh, "Estimation of the necessary number of points in riemannian voronoi," in *Proceedings of CCCG*, pp. 19–24, 2003.

[206] R. Osada, T. Funkhouser, B. Chazelle, and D. Dobkin, "Shape distributions," *ACM Transactions on Graphics*, vol. 21, no. 4, pp. 807–832, 2002.

[207] S. Osher and J. Sethian, "Fronts propagating with curvature-dependent speed: Algorithms based on Hamilton-Jacobi formulations," *Journal of Computational Physics*, vol. 79, pp. 12–49, 1988.

[208] S. J. Osher and R. Fedkiw, *Level Set Methods and Dynamic Implicit Surfaces*. Springer, 2002.

[209] S. J. Osher and N. Paragios, *Geometric Level Set Methods in Imaging, Vision, and Graphics*. Springer-Verlag, July 2003.

[210] V. Ostromoukhov, "A simple and efficient error-diffusion algorithm," in *Proceedings of SIGGRAPH*, pp. 567–572, 2001.

[211] V. Ostromoukhov, "Sampling with polyominoes," *ACM Transactions on Graphics*, vol. 26, no. 3, pp. 78–1–78–6, 2007.

[212] V. Ostromoukhov, C. Donohue, and P.-M. Jodoin, "Fast hierarchical importance sampling with blue noise properties," *ACM Transactions on Graphics*, vol. 23, no. 3, pp. 488–495, August 2004.

[213] N. Paragios, Y. Chen, and O. D. Faugeras, *Handbook of Mathematical Models in Computer Vision*. Springer, 2005.

[214] M. Péchaud, “Shortest paths calculations, and applications to medical imaging,” PhD thesis, Université Paris 7/ENS/ENPC, September 2009.
[215] M. Péchaud, M. Descoteaux, and R. Keriven, “Brain connectivity using geodesics in hardi,” in *MICCAI*, London, England, September 2009.
[216] M. Péchaud, G. Peyré, and R. Keriven, “Extraction of tubular structures over an orientation domain,” in *CVPR’09: Proceedings of the 2009 IEEE Computer Society Conference on Computer Vision and Pattern Recognition*, Washington, DC, USA: IEEE Computer Society, 2009.
[217] X. Pennec, “Intrinsic statistics on riemannian manifolds: Basic tools for geometric measurements,” *Journal of Mathematical Imaging and Vision*, vol. 25, no. 1, pp. 127–154, 2006.
[218] G. Peyré and L. Cohen, “Heuristically driven front propagation for fast geodesic extraction,” *International Journal for Computational Vision and Biomechanics*, vol. 1, no. 1, 2007.
[219] G. Peyré and L. D. Cohen, “Surface segmentation using geodesic centroidal tesselation,” in *Proceedings of 3DPVT*, pp. 995–1002, IEEE Computer Society, 2004.
[220] G. Peyré and L. D. Cohen, *Progress in Nonlinear Differential Equations and Their Applications,* vol. 63, chapter Geodesic Computations for Fast and Accurate Surface Remeshing and Parameterization, pp. 157–171. Birkhauser, 2005.
[221] G. Peyré and L. D. Cohen, “Geodesic remeshing using front propagation,” *International Journal of Computer Vision*, vol. 69, no. 1, pp. 145–156, 2006.
[222] S. Pippa and G. Caligiana, “Gradh-correction: Guaranteed sizing gradation in multi-patch parametric surface meshing,” *International Journal for Numerical Methods in Engineering*, vol. 62, no. 4, pp. 495–515, 2004.
[223] I. Pohl, “Bi-directional search,” in *Machine Intelligence,* vol. 6, (B. Meltzer and D. Michie, eds.), pp. 124–140, Edinburgh University Press, 1971.
[224] K. Polthier and M. Schmies, “Straightest geodesics on polyhedral surfaces,” in *Mathematical Visualization*, (H.-C. Hege and K. Polthier, eds.), pp. 135–150, Springer Verlag, 1998.
[225] K. Polthier and M. Schmies, “Geodesic flow on polyhedral surfaces,” in *Data Visualization˜’99*, (E. Gröller, H. Löffelmann, and W. Ribarsky, eds.), pp. 179–188, Springer-Verlag Wien, 1999.
[226] K. Polthier and M. Schmies, “Straightest geodesics on polyhedral surfaces,” in *SIGGRAPH ’06: ACM SIGGRAPH 2006 Courses*, pp. 30–38, New York, NY, USA: ACM, 2006.
[227] M. Poon, G. Hamarneh, and R. Abugharbieh, “Live-vessel: Extending livewire for simultaneous extraction of optimal medial and boundary paths in vascular images,” in *Proceedings of MICCAI (2)*, pp. 444–451, 2007.
[228] A. M. Popovici and J. A. Sethian, “3-d imaging using higher order fast marching traveltimes,” *Geophysics*, vol. 67, no. 2, pp. 604–609, 2007.
[229] H. Pottmann, J. Wallner, Q.-X. Huang, and Y.-L. Yang, “Integral invariants for robust geometry processing,” *Computer Aided Geometric Design*, vol. 26, no. 1, pp. 37–60, 2009.

[230] E. Prados, F. Camilli, and O. Faugeras, "A unifying and rigorous shape from shading method adapted to realistic data and applications," *Journal of Mathematical Imaging and Vision*, vol. 25, no. 3, pp. 307–328, 2006.

[231] E. Prados, C. Lenglet, J.-P. Pons, N. Wotawa, R. Deriche, O. Faugeras, and S. Soatto, "Control theory and fast marching techniques for brain connectivity mapping," in *Proceedings of the IEEE Conference on Computer Vision and Pattern Recognition, New York, NY, June, 2006,* vol. 1, pp. 1076–1083, IEEE, June 2006.

[232] W. H. Press, et al, *Numerical Recipes in C: The Art of Computer Programming*. Cambridge University Press, 1988.

[233] R. J. Prokop and A. P. Reeves, "A survey of moment-based techniques for unoccluded object representation and recognition," *CVGIP: Graphical Models and Image Processing*, vol. 54, no. 5, pp. 438–460, September 1992.

[234] J. Qian, Y.-T. Zhang, and H.-K. Zhao, "Fast sweeping methods for eikonal equations on triangulated meshes," *SIAM Journal on Numerical Analysis*, vol. 45, pp. 83–107, 2007.

[235] J. Rabin, G. Peyré, and L. D. Cohen, "Geodesic shape retrieval via optimal mass transport," in *Proceedings of ECCV'10*, pp. 48–57, 2010.

[236] J. Reif and Z. Sun, "Movement planning in the presence of flows," *Algorithmica*, vol. 39, no. 2, pp. 127–153, 2004.

[237] M. Reuter, F.-E. Wolter, and N. Peinecke, "Laplace-spectra as fingerprints for shape matching," in *Symposium on Solid and Physical Modeling*, (L. Kobbelt and V. Shapiro, eds.), pp. 101–106, ACM, 2005.

[238] J. Rickett and S. Fomel, "A second-order fast marching eikonal solver," January 13 2000.

[239] S. Rippa, "Long and thin triangles can be good for linear interpolation," *SIAM Journal on Numerical Analysis*, vol. 29, no. 1, pp. 257–270, February 1992.

[240] A. Rosenfeld and J. L. Pfaltz, "Distance functions on digital pictures," *Pattern Recognition*, vol. 1, no. 1, pp. 33–61, 1968.

[241] G. Rosman, A. M. Bronstein, M. M. Bronstein, A. Sidi, and R. Kimmel, "Fast multidimensional scaling using vector extrapolation," Technical Report CIS-2008-01, Department of Computer Science, Technion, Israel, 2008.

[242] G. Rosman, M. M. Bronstein, A. M. Bronstein, and R. Kimmel, "Nonlinear dimensionality reduction by topologically constrained isometric embedding," *International Journal of Computer Vision*, vol. 8, no. 1, pp. 56–68, 2010.

[243] J. R. Rossignac and A. A. G. Requicha, "Offsetting operations in solid modeling," *Computer Aided Design*, vol. 3, no. 2, pp. 129–148, August 1986.

[244] E. Rouy and A. Tourin, "A viscosity solutions approach to shape-from-shading," *SIAM Journal on Numerical Analysis*, vol. 29, no. 3, pp. 867–884, 1992.

[245] S. T. Roweis and L. K. Saul, "Nonlinear dimensionality reduction by locally linear embedding," *Science*, vol. 290, no. 5500, pp. 2323–2326, December 2000.

[246] Y. Rubner, C. Tomasi, and L. J. Guibas, "The earth mover's distance as a metric for image retrieval," *International Journal of Computer Vision*, vol. 40, no. 2, pp. 99–121, November 2000.

[247] J. Ruppert, "A Delaunay refinement algorithm for quality 2-dimensional mesh generation," *Journal of Algorithms*, vol. 18, no. 3, pp. 548–585, 1995.
[248] T. Saito and J. I. Toriwaki, "New algorithms for Euclidean distance transformation of an n-dimensional digitized picture with applications," *Pattern Recognition*, vol. 27, no. 11, pp. 1551–1565, 1994.
[249] A. Schrijver, *Combinatorial Optimization: Polyhedra and Efficiency,* vol. A, Paths, Flows, Matchings, Chapter 1–38. Springer, Schrijver, 2003.
[250] E. L. Schwartz, A. Shaw, and E. Wolfson, "A numerical solution to the generalized mapmaker's problem: Flattening nonconvex polyhedral surfaces," *IEEE Transactions on Pattern Analysis and Machine Intelligence*, vol. 11, no. 9, pp. 1005–1008, 1989.
[251] T. B. Sebastian, P. N. Klein, and B. B. Kimia, "On aligning curves," *IEEE Transactions on Pattern Analysis and Machine Intelligence*, vol. 25, no. 1, pp. 116–124, January 2003.
[252] T. B. Sebastian, P. N. Klein, and B. B. Kimia, "Recognition of shapes by editing their shock graphs," *IEEE Transactions on Pattern Analysis and Machine Intelligence*, vol. 26, no. 5, pp. 550–571, May 2004.
[253] J. Serra, *Image Analysis and Mathematical Morphology.* Orlando, FL, USA: Academic Press, Inc., 1983.
[254] J. A. Sethian, "A fast marching level set method for monotonically advancing fronts," *Proceedings of the National Academy of Sciences*, vol. 93, no. 4, pp. 1591–1595, 1996.
[255] J. A. Sethian, *Level Sets Methods and Fast Marching Methods.* Cambridge University Press, 2nd Edition, 1999.
[256] J. A. Sethian and A. Vladimirsky, "Ordered upwind methods for static Hamilton–Jacobi equations: Theory and algorithms," *SIAM Journal on Numerical Analysis*, vol. 41, no. 1, pp. 325–363, 2003.
[257] A. Sheffer, E. Praun, and K. Rose, "Mesh parameterization methods and their applications," *Foundations and Trends in Computer Graphics and Vision*, vol. 2, no. 2, 2006.
[258] J. R. Shewchuk, "Delaunay refinement algorithms for triangular mesh generation," *Computational Geometry*, vol. 22, nos. 1–3, pp. 21–74, 2002.
[259] J. R. Shewchuk, "What is a good linear element? Interpolation, conditioning, and quality measures," in *International Meshing Roundtable*, pp. 115–126, 2002.
[260] F. Y. Shih and Y. T. Wu, "The efficient algorithms for achieving euclidean distance transformation," *IEEE Transactions on Image Processing*, vol. 13, no. 8, pp. 1078–1091, August 2004.
[261] F. Y. Shih and Y. T. Wu, "Fast euclidean distance transformation in two scans using a 3×3 neighborhood," *Computer Vision and Image Understanding*, vol. 93, no. 2, pp. 195–205, February 2004.
[262] E. Sifakis, C. Garcia, and G. Tziritas, "Bayesian level sets for image segmentation," *Journal of Visual Communication and Image Representation*, vol. 13, nos. 1/2, pp. 44–64, March 2002.
[263] A. Spira and R. Kimmel, "An efficient solution to the eikonal equation," *Interfaces and Free Boundaries*, vol. 6, no. 3, pp. 315–327, 2004.

[264] V. Surazhsky, T. Surazhsky, D. Kirsanov, S. J. Gortler, and H. Hoppe, "Fast exact and approximate geodesics on meshes," *ACM Transactions on Graphics*, vol. 24, no. 3, pp. 553–560, 2005.

[265] M. Tang, M. Lee, and Y. J. Kim, "Interactive hausdorff distance computation for general polygonal models," in *Proceedings of SIGGRAPH'09*, pp. 1–9, New York, NY, USA: ACM, 2009.

[266] J. W. H. Tangelder and R. C. Veltkamp, "A survey of content based 3D shape retrieval methods," *Multimedia Tools and Applications*, vol. 39, no. 3, pp. 441–471, 2008.

[267] M. Teague, "Image analysis via the general theory of moments," *Journal of the Optical Society of America*, vol. 70, no. 8, pp. 920–930, August 1980.

[268] C. H. Teh and R. T. Chin, "On image analysis by the methods of moments," *IEEE Transactions on Pattern Analysis and Machine Intelligence*, vol. 10, no. 4, pp. 496–513, July 1988.

[269] A. Telea and J. J. van Wijk, "An augmented fast marching method for computing skeletons and centerlines," in *Proceedings of the symposium on Data visualisation 2002*, (D. Ebert, P. Brunet, and I. Navazo, eds.), pp. 251–259, Barcelona, Spain: Eurographics Association, 2002.

[270] J. B. Tenenbaum, V. de Silva, and J. C. Langford, "A global geometric framework for nonlinear dimensionality Reduction," *Science*, vol. 290, no. 5500, pp. 2319–2323, December 2000.

[271] N. Thorstensen and R. Keriven, "Non-rigid shape matching using geometry and photometry," in *Proceedings of ACCV*, 2009.

[272] L. Torresani, V. Kolmogorov, and C. Rother, "Feature correspondence via graph matching: Models and global optimization," in *Proceedings of ECCV*, pp. 596–609, 2008.

[273] A. Treuille, S. Cooper, and Z. Popović, "Continuum crowds," *ACM Transactions on Graphics*, vol. 25, no. 3, pp. 1160–1168, 2006.

[274] A. Trouve and L. Younes, "Diffeomorphic matching problems in one dimension: Designing and minimizing matching functionals," in *Proceedings of ECCV,* vol. I, pp. 573–587, 2000.

[275] Y.-H. R. Tsai, L.-T. Cheng, S. Osher, and H.-K. Zhao, "Fast sweeping algorithms for a class of Hamilton–Jacobi equations," *SIAM Journal on Numerical Analysis*, vol. 41, no. 2, pp. 673–694, April 2003.

[276] J. Tsitsiklis, "Efficient algorithms for globally optimal trajectories," *IEEE Transactions on Automatic Control*, vol. 40, no. 9, pp. 1528–1538, September 1995.

[277] W. T. Tutte, "How to draw a graph," *Proceedings of London Mathematic*, vol. 13, pp. 743–768, 1963.

[278] S. Valette, J. M. Chassery, and R. Prost, "Generic remeshing of 3D triangular meshes with metric-dependent discrete Voronoi diagrams," *IEEE Transactions on Visualization and Computer Graphics*, vol. 14, no. 2, pp. 369–381, 2008.

[279] R. Van Uitert and I. Bitter, "Subvoxel precise skeletons of volumetric data based on fast marching methods," *Medical physics*, vol. 34, pp. 627–638, 2007.

[280] R. C. Veltkamp, "Shape matching: Similarity measure and algorithms," in *Proceedings Shape Modelling International*, pp. 188–197, IEEE Press, 2001.

[281] R. C. Veltkamp and L. J. Latecki, "Properties and performance of shape similarity measures," in *Proceedings of the 10th IFCS Conference on Data Science and Classification*, Slovenia, July 2006.

[282] C. Villani, *Topics in Optimal Transportation*. American Mathematical Society, 2003.

[283] L. Vincent and P. Soille, "Watersheds in digital spaces: An efficient algorithm based on immersion simulations," *IEEE Transactions on Pattern Analysis and Machine Intelligence*, vol. 13, no. 6, pp. 583–598, 1991.

[284] D. Wagner and T. Willhalm, "Geometric speed-up techniques for finding shortest paths in large sparse graphs," in *Proceedings of ESA*, vol. 2832, (G. D. Battista and U. Zwick, eds.), pp. 776–787, Springer, 2003.

[285] C. Wang, M. M. Bronstein, and N. Paragios, "Discrete minimum distortion correspondence problems for non-rigid shape matching," *INRIA Report,* 7333, 2010.

[286] J. G. Wardrop, "Some theoretical aspects of road traffic research," *Proceedings — Institution of Civil Engineers*, vol. 2, no. 2, pp. 325–378, 1952.

[287] O. Weber, Y. S. Devir, A. M. Bronstein, M. M. Bronstein, and R. Kimmel, "Parallel algorithms for approximation of distance maps on parametric surfaces," *ACM Transactions on Graphics*, vol. 27, no. 4, no. 4, 2008.

[288] J. W. J. Williams, "Algorithm 232: Heapsort," *Communications of the ACM*, vol. 7, pp. 347–348, 1964.

[289] L. R. Williams and D. W. Jacobs, "Stochastic completion fields: A neural model of illusory contour shape and salience," *Neural Computation*, vol. 9, no. 4, pp. 837–858, 1997.

[290] E. Wolfson and E. L.Schwartz, "Computing minimal distances on polyhedral surfaces," *IEEE Transactions on Pattern Analysis and Machine Intelligence*, vol. 11, no. 9, pp. 1001–1005, 1989.

[291] R. P. Woods, "Characterizing volume and surface deformations in an atlas framework: Theory, applications, and implementation," *NeuroImage*, vol. 18, no. 3, pp. 769–788, 2003.

[292] S. Yamakawa and K. Shimada, "High quality anisotropic tetrahedral mesh generation via ellipsoidal bubble packing," in *9th International Meshing Roundtable*, pp. 263–274, 2000.

[293] L. Yatziv, A. Bartesaghi, and G. Sapiro, "O(n) implementation of the fast marching algorithm," *Journal of Computational Physics*, vol. 212, no. 2, pp. 393–399, 2006.

[294] Y. Yokosuka and K. Imai, "Guaranteed-quality anisotropic mesh generation for domains with curves," in *Proceedings of EWCG'06*, 2006.

[295] C. T. Zahn and R. Z. Roskies, "Fourier descriptors for plane closed curves," *IEEE Transactions on Computer*, vol. 21, no. 3, pp. 269–281, March 1972.

[296] D. S. Zhang and G. J. Lu, "Review of shape representation and description techniques," *Pattern Recognition*, vol. 37, no. 1, pp. 1–19, January 2004.

[297] R. Zhang, P.-S. Tsai, J. E. Cryer, and M. Shah, "Shape from shading: A survey," *IEEE Transactions on Pattern Analysis and Machine Intelligence*, vol. 21, no. 8, pp. 690–706, 1999.

[298] H. Zhao, "Parallel implementations of the fast sweeping method," *Journal of Computational Mathematics*, vol. 25, no. 4, pp. 421–429, 2007.

[299] L. Zhou, M. S. Rzeszotarski, L. J. Singerman, and J. M. Chokreff, "The detection and quantification of retinopathy using digital angiograms," *IEEE Transactions on Medical Imaging*, vol. 13, no. 4, pp. 619–626, 1994.

[300] S. C. Zhu, "Stochastic jump-diffusion process for computing medial axes in markov random fields," *IEEE Transactions on Pattern Analysis and Machine Intelligence*, vol. 21, no. 11, pp. 1158–1169, November 1999.

[301] S. C. Zhu and A. L. Yuille, "FORMS: A flexible object recognition and modelling system," *International Journal of Computer Vision*, vol. 20, no. 3, pp. 187–212, 1996.

[302] G. Zigelman, R. Kimmel, and N. Kiryati, "Texture mapping using surface flattening via multi-dimensional scaling," *IEEE Transactions on Visualization and Computer Graphics*, vol. 8, no. 1, pp. 198–207, 2002.